Appendix 1

List of participants

Participants EFC WP15 meeting 8th April 2014 Mechelen (Belgium)

Name	Company	Country
Deborah Heritier	Arcelor Mittal	FRANCE
Sylvain Pillot	Arcelor Mittal	FRANCE
Francesco Ciccomascolo	Böhler Welding Holding GmbH	GERMANY
Gino De Landtsheer	Borealis	BELGIUM
Piet Van Dooren	Borealis	BELGIUM
Frederic Tabaud	BP R&LT	NETHERLANDS
Stine Hals Verstraelen	CB&I Lummus B.V.	NETHERLANDS
John Houben	ExxonMobil Chemical Holland BV	NETHERLANDS
Claudia Lavarde	GE Measurement & Control	FRANCE
Johan Van De Vijvere	GE Measurement & Control	FRANCE
Swen Koller	Holborn Europa Raffinerie GmbH	GERMANY
Francois Ropital	IFP Energies nouvelles	FRANCE
Chris J Claesen	Nalco	BELGIUM
Valerie Bour Beucler	Nalco Energy Services	FRANCE
Christoph Scharsching	OMV Refining & Marketing GmbH	AUSTRIA
Stephen Fenton	Performance Polymers b.v	NETHERLANDS
Steve Reynolds	Performance Polymers b.v	NETHERLANDS
Maria Jose Yanes Guardado	REPSOL	SPAIN
Hennie de Bruyn	Saudi Aramco	SAUDI ARABIA
Chretien Hermse	Shell Global Solutions International	NETHERLANDS
Johan van Roij	Shell Global Solutions International	NETHERLANDS
Tracey Holmes	Special Metals	UK
Steve Mc Coy	Special Metals / PCC energy EP	UK
Stein Brendryen	Statoil ASA	NORWAY
Fred Van Rodijnene	Sulzer Metco Europe GmbH	GERMANY
Stefan Winnik	SW Materials And Corrosion Ltd	UK
Johan Sentjens	Temati	NETHERLANDS
Christel Augustin	Total Refining & Chemicals	FRANCE
François Dupoiron	Total Refining & Chemicals	FRANCE
Martin Richez	Total Refining & Chemicals	FRANCE
Jean Pierre Van Nieuwenhoven	Voestalpine Böhler welding Belgium	BELGIUM

Appendix 2

EFC WP15 Activities

(F. Ropital)

Presentation of the activities of WP15

European Federation of Corrosion (EFC)

- Federation of 31 National Associations
- 20 Working Parties (WP)
- Annual Corrosion congress « Eurocorr »
- Thematic workshops and symposiums
- Working Party meetings (for WP15 twice a year)
- Publications
- EFC - NACE agreement (20% discount on books price)
- for more information http://www.efcweb.org

EFC Working Party 15 « Corrosion in Refinery » Activities

http://www.efcweb.org/Working+Parties-p-104085/WP%2B15-p-104111.html

Chairman: Francois Ropital Deputy Chairman: Hennie de Bruyn

The following are the main areas being pursued by the Working Party:

Information Exchange
Sharing of refinery materials /corrosion experiences by operating company representatives.

Forum for Technology
Sharing materials/ corrosion/ protection/ monitoring information by providers

Eurocorr Conferences

WP Meetings
One WP 15 working party meeting in Spring,
One meeting at Eurocorr in September in conjunction with the conference,

Publications - Guidelines

EFC Working Party 15 « Corrosion in Refinery »

List of the WP15 spring meetings :

10 April 2003	Pernis - NL (Shell)
8-9 March 2004	Milan -Italy (ENI)
17-18 March 2005	Trondheim- Norway (Statoil)
31 March 2006	Porto Maghera - Italy (ENI)
26 April 2007	Paris - France (Total)
15 April 2008	Leiden -NL (Nalco)
23 April 2009	Vienna - Austria (Borealis)
22 June 2010	Budapest - Hungary (MOL)
14 April 2011	Paris - France (EFC Head offices)
26 April 2012	Amsterdam - NL (Shell)
9 April 2013	Paris - France (Total)

Publications from WP15

- EFC Guideline n°40 « Prevention of corrosion by cooling waters » available from http://www.woodheadpublishing.com/en/book.aspx?bookID=1193

Update in relation with Nace document 11106 "Monitoring and adjustment of cooling water treatment operating parameters" Task Group 152 on cooling water systems

- EFC Guideline n° 46 on corrosion in amine units http://www.woodheadpublishing.com/en/book.aspx?bookID=1299

- EFC Guideline n° 42 Collection of selected papers http://www.woodheadpublishing.com/en/book.aspx?bookID=1295

- EFC Guideline n° 55 Corrosion Under Insulation http://www.woodheadpublishing.com/en/book.aspx?bookID=1486

- Future publications : suggestions ?
  - best practice guideline to avoid and characterize stress relaxation cracking ?

EFC Working Party 15 plan work 2014-2016

. Collaboration with Nace : exchange of minutes of meetings TEG 205X, co-organisation of conference (BOTH Nov. 2013 in Frankfurt), …

. Sessions with other EFC WP at Eurocorr (2014 Pisa-Italy, 2015 Graz-Austria, 2016-Montpellier-France) on which topics?

High temperature corrosion with WP3 during Eurocorr 2014

For the next Eurocorr ?

- Update of publications
  - CUI guideline

- New Publications: best practice guideline to avoid and characterize stress relaxation cracking ?

- Education – qualification – certification

List of "corrosion refinery" related courses on EFC website ?

Proposal of courses within Eurocorr ?

WP15 Corrosion Atlas Web page

http://www.efcweb.org/Working+Parties/WP+Corrosion+in+the+Refinery+Industry/WP+15+Refinery+Corrosion+Atlas.html

Thank you to Martin Hofmeister for proposing a new case (n°9)

Eurocorr 2014

Pisa 9-12 September 2014

Authors have been informed by mid April

Refinery corrosion session with 13 oral presentations and 10 posters
(Wednesday 10 Sept – to be confirmed)

Joint session with WP13 on high temperature corrosion with 4 oral presentations
(Wednesday 10 Sept – to be confirmed)

Annual WP15 working party meeting during Eurocorr
(date to be fixed: Tuesday 9 September afternoon – to be confirmed)

http://www.eurocorr2013.org/?page=default

Information :
Future conferences related to refinery corrosion

•9-12 September 2014
EUROCORR 2014 Pisa Italy Website: www.efcweb.org/Events

•15-19 March 2015
Nace Conference 2015 Dallas USA

•6-10 September 2015
EUROCORR 2015 Gratz Austria

Appendix 3

Information on the JIP on Stress Relaxation Cracking

(F. Dupoiron)

Joint Industrial Research Programme:
Stress Relaxation Cracking

First Progress Report

Reference number: SRC/2013-1

Date: 23/10/2013

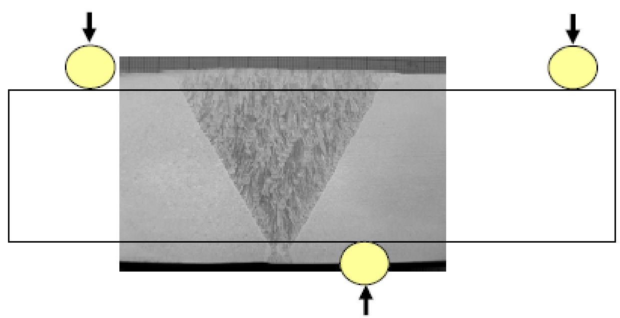

An example of the loading conditions in the 3-point bending test rig, used at TNO, to assess the relaxation performance of a welded joint.

In this case the maximum load is at the fusion line of the cap of the weld.

CONTENTS

1. Project partners

Status participants within the JIP programme:
Stress Relaxation Cracking (SRC)
Date: 21-11-2013

	Company	Contact person(s)
1	Borsig	J. Blum
2	CBI Lummus	J. Baas
3	Laborelec	S. Huysmans
4	NEM	P.de Smet / R. Radoux
5	Nippon Steel & Sumitomo Metal Corporation	H.Ogawa
6	Technip Benelux b.v.	E.Korner / C.van Straaten
7	Uhde	R. Kremer
8	ThyssenKruppVDM	H Hattendorf / J. van Lith
9	BASF	K. Schneider / J. Korkhaus
10	Böhler Welding	M. Schmitz Niederau
11	Dupont	L. Rose / D. Bakker
12	Haldor Topsoe	Maria Oestergaard
13	Johnson Matthey	G. Lobley
14	Linde	K. Koepf
15	Sabic	H. Schrijen / Mohammed Saad Al Rabie
16	Schmidt & Clemens	D. Jakobie / W. Hartnagel
17	Shell Global Solutions	W. Hamer / T. Wolfert / M.Church
18	Total	F. Dupoiron
19	Fluor	J.W. Rensman /C. Shargay
20	Arcelor Mital	A.Fanica
21	CMI	C. Fraikin
22	Special Metals	T. Holmes
23	Manoir Industries	B. Fournier
24	Petrobras	C. Raunich
25	Verolme Special Equipment	R.v.d Berg / C.v.d. Mast
26	Air Liquide	J. Furtado
27	Yara	A.de Bruijne

- Work Package 1 - Refinement of Recommended Practice;
  Goal:
  An improved Recommended Practice for a risk assessment on the occurrence of stress relaxation cracking by including the (local) stress intensity factor(s).

-

- Work Package 2 - Physico-Chemical and Micro-Mechanical Modelling of SRC;
  Goals:
  - Get a better understanding of the key micro scale parameters for the occurrence of stress relaxation cracking. This knowledge will be used as input for WP 1 in order to optimise the TNO remediation procedure.
  - Identify the most significant processes & parameters to formulate remedies and strategies to avoid, delay or reduce SRC in practice.

- Work Package 3 - Alternative remediation strategies;
  Goals:
  - Investigating the effect of alternative remediation strategies which are not based on heat treatment and can be used to treat new and existing components on site.
  - Assessing the effects on the occurrence of SRC by changing the heat treatment temperature and adjusting the heating/cooling rate during the SRC remediation procedure by TNO.

- Work Package 4 - Effect of stabilising heat treatment on creep life time;
  Goals:
  - Measuring the difference in creep strength of alloys 800H in the as-delivered state and the heat-treated 800H state in accordance with the TNO remediation procedure.
  - Assessing the information and/or guidelines that notified bodies need to have such that the creep reduction factor can be increased or even removed.

- Work Package 5 - Sensitivity to and prevention of SRC in new alloys and weldments;
  Goals:
  - Investigating the susceptibility to stress relaxation cracking of new alloys in accordance with the currently available "yes/no" susceptibility stress relaxation cracking assessment method.
  - Determination of the appropriate heat treatment procedure to prevent stress relaxation cracking of these new alloys.

- Work Package 6 - Stress relaxation cracking in dissimilar welded materials.
  Goals:
  - Assessing 2 types of dissimilar welds on their susceptibility to *SRC*.
  - Exploring the best remediation practices for reducing stress relaxation cracking in dissimilar welds by means of an effective:
    - Remediation heat treatment;
    - Alternative treatment as described in work package 3[1].

- Work Package 7 – Dissemination
  Goal:
  - To spread (some of) the knowledge about stress relaxation cracking outside the original industrial consortium into the rest of the world industrial partners (end users, engineering companies, material suppliers, vessel manufacturers, etc.).

4. Status of the programme

4.1 Work Package 1: Refinement of Recommended Practice.

A survey/questionnaire has been set up and distributed to the partners of the programme, see **Appendix 1**.
Up till now we received a response from Sabic, Yara, CBI Lummus, Technip and Uhde.
Totally 29 relaxation cracking failures were encountered in a variety of materials and operating conditions.

Progress

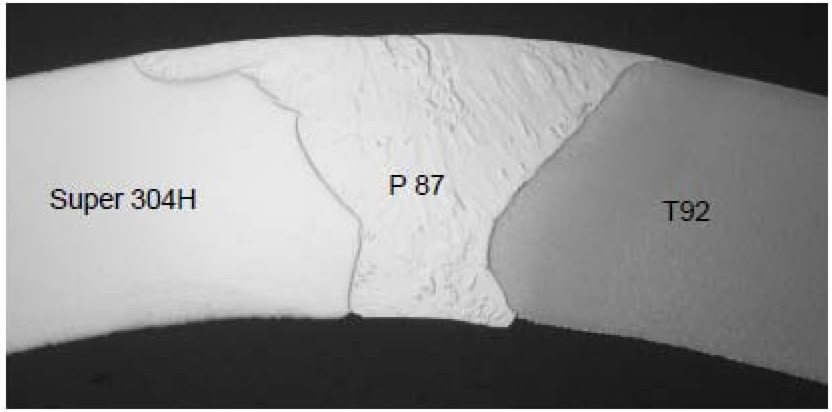

Figure 5: *Sample L1. Section in length of the tube after the relaxation test at 580°C. No relaxation damage was addressed.*

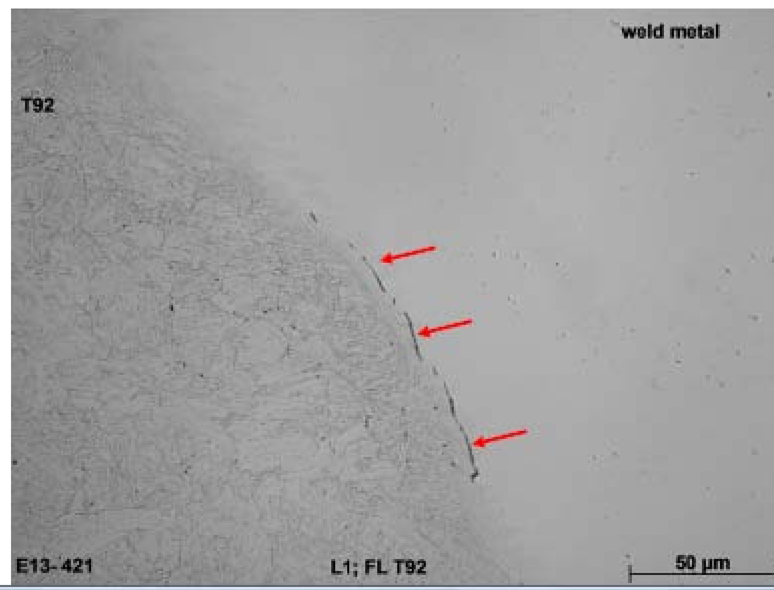

Proposed welded joints to be tested

Defined welded joints:

Weld	Base metal: side A	Weld metal
1	Tube centricast 20Cr32NiNb	21Cr 33Ni Mn
Delivered by:		
2	Tube centricast 20Cr32 NiNb	Alloy 82 or 21Cr 33Ni Mn or 617
Delivered by:		
3	Tube wrought super 304H	Matching
Delivered by:		
4	Tube DMV304H Cu (super 304H), 45 * 9.2 mm	P87
5	Tube super 304H 45 * 9.7	INCO 82 or P87
Delivered by:		

Weld	Base metal: side A	Weld metal
6	Plate wrought Alloy 800H	21Cr 33Ni Mn
Delivered by:		
7	Plate 617 (= with low B)	Matching
Delivered by:		
8	Plate 617 B (Nicrofer 5520 CoB) = with higher B	Matching
Delivered by:		
9	Plate C263	Matching?
Delivered by:		
10	Plate HR6W	Matching
Delivered by:		
11	Alloy 740H	Matching
Delivered by:		
12	Alloy 803	Matching?
Delivered by:		

Weld	Base metal: side A	Weld metal
13 A	Static cast Manoir 900	21Cr 33Ni Mn
Delivered by:		
13 B	Static cast Manoir 900	Alloy 617
Delivered by:		
13 C	Tube centricast Manoir 900	21Cr 33Ni Mn r
Delivered by:		
13 D	Tube centricast Manoir 900	Alloy 617 r
Delivered by:	Manoir	
14	Plate AC66 (Nicrofer 3228 Nb)	Nicrofer S 3228 TIG
Delivered by:		
15	Plate Alloy 690 (Nicrofer 630)	UTP 6229 Mn
Delivered by:		g
16	Plate Alloy 625 (Nicrofer 6020 hMo)	UTP 6222 Mo Sa t
Delivered by:		g
17	Tube 347H (segment) Heat 44642	347H
Delivered by:		

Thank you for your attention

For partners : think to answer to the survey

For the other … Join the JIP

Appendix 5

New heat exchanger materials

(V. Bour Beucler)

Impact of new materials on cooling water systems

Eurocorr 2014

Mechelen Spring Meeting

Valerie Bour Beucler

NALCO Champion
An Ecolab Company

Cooling water system successful management

- Cooling water successfull management
  - A good equilibrium between corrosion, scaling and MIC

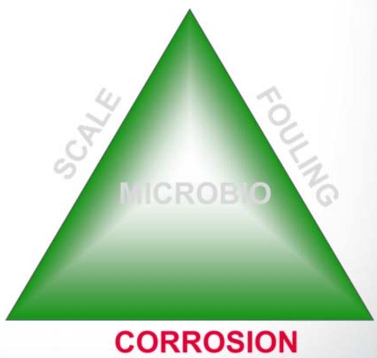

Regulation and cooling system

- **Legionella Control and regulation**
  - Minimize the risk of legionella
- **Biocidal Product Directive / Regulation**
  - harmonise the European market for biocidal products and their active substances.
- **REACH (European Commity Regulation on Chemical and their safe Use (EC 1907/2006)**
  - It deals the Registration Evaluation Authorisation and Restriction of Chemical substances.
- **The Future**
  - **Less non oxidizing biocides**
  - **More oxidizing biocide but with AOX control**
    - **Chlorine dioxide (ClO_2), a good alternative**

Impact of bleach uses as biocide on cooling system

- Couldn't penetrate by itself the biofilm
  - Biodetergent addition
- Loss of effectiveness at higher pH
- Reacts with the cooling water programs as azoles
- Byproduct **AOX or THMs** after hydrocarbon leaks
- Increases yellow metals corrosion rate
- Could generate copper galvanic corrosion on carbon steel.
  - Increase iron fouling and contamination

Why is ClO_2 a Good Biocide?

- It's a gas that is highly soluble in water, **diffuses into biofilms** attacking the bacteria generating the biofilm
- It doesn't hydrolyze like chlorine gas or bleach: **no loss of effectiveness at higher pH**
- It is non-reactive to most organics and ammonia
  - No loss of biocide effectiveness due to byproduct reaction
  - **Doesn't react with the cooling water program (azoles)**
- No byproduct **AOX or THMs** afterhydrocarbon leaks.

Typically 10-40% of the bleach requirement

M.O.C. Audit a very important tool….

MECHANICAL	OPERATIONAL	CHEMICAL
Exchanger Data	**Control Analysis**	**Scaling Modeling** **Corrosion Modeling**
Skin Temperature **Water Velocity** **Heat Flux**	**Histogram** **Control Chart** **Process Capability**	**Model Scaling Tendencies** **Model Inhibitor Dosages** **Vary Temp, Cycles, MU Source**
Determine Thermal Limits **Hydraulic Upgrade** **Identify Problem Areas**	**Determine Control Capabilities** **Identify Control Problems** **Justify Automation**	**Determine Control Limits** **Determine Treatment Demand** **Justify MU Alternatives**
Metallurgy		

Stress Factors Associated with Problem Exchangers

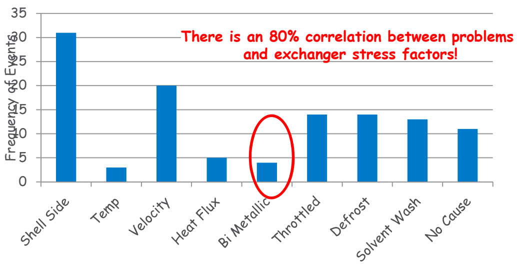

- Operating conditions
- Type of construction
- Metallurgy
- Position

Mechanical stress parameters

Low velocity

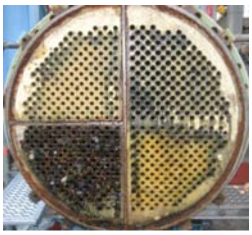

Operational parameters	Low	Moderate	High	Severe
Skin Temperature (^oC)	< 50	50 – 60	60 – 70	➢70
Velocity (ms^{-1})	➢1	0.6 – 1.0	0.6 – 0.3	< 0.3
Heat Flux ($MJm^{-2}.hr^{-1}$)	< 25	25 - 50	50 - 75	> 75
Chemical parameters				
Langelier	< 0.5	0.5 – 1.5	1.5 – 2.5	➢2.5
Ryznar	➢6.0	4.5 – 6.0	3.5 – 4.5	< 3.5
TCP SSI	< 20	20 –1000	1000 – 1500	>1500
Iron (mgl^{-1})	< 1.0	1.0 – 3.0	3.0 – 5.0	➢5.0

Increase corrosion and scaling risk

Metallurgy

- **Copper materials**
  - **Galvanic corrosion on carbon steel**

Tube sheet in CS
Tubes in Copper

- **Duplex stainless steel**
  - **Increase of Duplex parts of heat exchangers**
  - **Increase of galvanic corrosion on carbon steel**

Shell in carbon steel
Tubes in Duplex

Increase of CS corrosion rate and iron contamination

Metallurgy

- **Stainless steel**
  - **Galvanic corrosion on carbon steel**

Tube sheet in CS
Rubber in stainless steel

Baffles in carbon steel
Tubes in AISI 304L

Increase of CS corrosion rate and iron contamination

New materials, galvanic corrosion and cooling system

- Corrosion inhibitor (yellow metal or carbon steel) couldn't prevent galvanic corrosion, particularly with stainless steel
- Direct contact between carbon steel and yellow metal or stainless steel should be avoided.
- Physical barrier should be proposed or implemented to stop direct contact between carbon steel and other metallurgy (yellow metal or stainless steel).
- Replacement of carbon steel tubes by duplex tubes could be an opportunity but engineering should review the heat exchangers design to minimize galvanic corrosion risks.

NALCO Champion
An Ecolab Company

Taking Energy Further™ 11

QUESTIONS

NALCO Champion
An Ecolab Company

12
1
2

Appendix 6

High Temperature Hydrogen Attack

Documents

A Qualitative Risk Based Procedure for HTHA of C-1/2 Mo Steel

Cracking of non-PWHT'd Carbon Steel Operating at Conditions Immediately Below the Nelson Curve

Proceedings of PVP2007-XXXXX11-26129
2007 ASME Pressure Vessels and Piping Conference
July 22-26, 2007, San Antonio, Texas

A Qualitative Risk-Based Assessment Procedure for High Temperature Hydrogen Attack of C-1/2Mo Steel

James E. McLaughlin
Distinguished Engineering Associate
ExxonMobil Research and Engineering Company
Fairfax, VA

ABSTRACT

A qualitative risk-based assessment procedure was developed to determine the relative probability of failure for high temperature hydrogen attack (HTHA) of C-1/2Mo steel. It is well documented that C-1/2Mo possesses a variable resistance to HTHA. Over the years, the Nelson curve limits, as published in API RP 941, Steels for Hydrogen Service at Elevated Temperatures and Pressures in Petroleum Refineries and Petrochemical Plants, have been significantly reduced since originally published. This has created a need for an assessment procedure to evaluate C-1/2 Mo equipment that was designed many years ago when the Nelson curve was at much higher operating conditions than today. This assessment procedure is based on the current ExxonMobil assignment of C-1/2Mo resistance to HTHA on the Nelson curve and the relative dependence of HTHA on temperature, hydrogen partial pressure and time. We use the Pv relationship that appears in literature to define the relative dependence of HTHA on temperature, hydrogen partial pressure and time. This qualitative assignment of probability levels for HTHA was validated against actual HTHA failures of C-1/2Mo in high temperature hydrogen service that have been reported to the API and other internal Company incidents not reported to API. This assessment procedure is used to qualitatively define the probability of failure consistent with the probability levels defined in the ExxonMobil risk matrix which is used to manage all risk based decisions in the Corporation.

INTRODUCTION

The assessment of high temperature hydrogen attack (HTHA) of C-1/2Mo has been very important during the last 25 years in the refining industry. It is well documented that C-1/2Mo possesses a variable resistance to HTHA[1]. Over the years, the Nelson curve limits, as published in API RP 941, Steels for Hydrogen Service at Elevated Temperatures and Pressures in Petroleum Refineries and Petrochemical Plants, have been significantly reduced since originally published in 1970. This has created a need for an assessment procedure to evaluate C-1/2 Mo equipment that was designed many years ago when the Nelson curve was at much higher operating conditions than today. This assessment procedure is based on the current ExxonMobil assignment of C-1/2Mo resistance to HTHA on the Nelson curve and the relative dependence of HTHA on temperature, hydrogen partial pressure and time. Our assessment procedure for HTHA is risk based and consistent with the ExxonMobil corporate risk matrix which is used to manage all risk based decisions in the Corporation.

The ExxonMobil risk matrix as shown in Figure 1 contains both a probability level and a consequence level for each risk we evaluate. We have shown the qualitative definitions for the probability categories. This paper will only address our procedure for evaluating the probability of failure associated with the risk based assessment. It should be noted there is more detailed information on the use of the risk matrix and description of each of the probability and consequence categories.

GUIDELINES FOR SETTING THE PROBABILITY OF FAILURE

HTHA is the result of a reaction of diffusible hydrogen in steel with metal carbides to form methane gas as shown by the following reaction.

$$\mathbf{MC\ (Carbide) + 2H_2 = M + CH_4}$$

As shown in literature[2] the Pv relationship provides the HTHA dependence on time at a specific hydrogen partial pressure and temperature. The Pv value for a steel essentially represents the metal's resistance to HTHA for a given time at a hydrogen partial pressure and temperature. Pv is defined as follows:

$$\mathbf{Pv = \log(H_2\ PP) + 3.09x10^{-4}x(T)x(\log(t) + 14)}$$

where: H_2 PP = hydrogen partial pressure in kg/cm^2
T = temperature in ^{o}K
t = time in hours

As mentioned earlier, there have been many failures of C-1/2Mo equipment in HTHA service operating at conditions above the Nelson curve limits for carbon steel but well below the original limits established for C-1/2Mo in earlier editions of API RP-941. As a result of these failures, the current edition of RP-941 does not provide any credit for the use of C-1/2Mo over carbon steel for new construction. However, the equipment owners still have to address the concern associated with existing C-1/2Mo equipment operating above the Nelson curve limits for carbon steel. As a result of this concern, ExxonMobil has developed a risk based assessment procedure for evaluating C-1/2Mo steel operating above the Nelson curve limits for carbon steel.

The first step in developing our assessment procedure was to evaluate the reported HTHA failures of C-1/2Mo. There were many HTHA failures reported to API and several investigated by ExxonMobil but not reported to API. Table 1 lists 11 HTHA failures of C-1/2Mo closest to the carbon steel curve. This table also provides a summary of reported conditions and damage for each of these failures. Based on our initial assessment of these reported failures we established an "effective Nelson curve" for the assessment of C-1/2Mo operating above the published carbon steel curve. This "effective Nelson curve" for C-1/2Mo is shown as the area in Figure 2 marked by the letter **E**. In the high hydrogen pressure regime of the curve it is 50°F (28°C) above the carbon steel line, while in the vertical portion of the curve it 20 psia (1.4 bara) above the carbon steel line. Essentially, operation in this area of the curve produced no reported failures of C-1/2Mo. As a Company, we established the curve defined by this area as the "revised C-1/2Mo Nelson" curve that we used for assessing existing equipment. Operation above this line, equipment was vulnerable and below this line equipment was no vulnerable.

Several years ago we established guidelines for defining the probability of failure from HTHA associated with operation above the curve. The rules we established were based on the probability categories in the ExxonMobil risk matrix shown in Figure 1. These rules which are illustrated on Figure 2 are as follows:

- 50°F (28°C) above the API RP-941 carbon steel curve - demarcation between E and D probability level
- 75°F (42°C) above the API RP-941 carbon steel curve - demarcation between D and C probability level
- 100°F (56°C) above the API RP-941 carbon steel curve - demarcation between C and B probability level
- 125°F (69°C) above the API RP-941 carbon steel curve - demarcation between B and A probability level

For points greater than 125°F (69°C) above the API RP-941 carbon steel curve, there is an A probability of failure due to HTHA.

DETERMINING THE PROBABILITY OF FAILURE FOR HTHA

Based on the defined probability levels shown in Figure 2 and using the Pv relationship for determining the time, temperature and hydrogen partial pressure dependence on HTHA, we have established an easy 2 step procedure for defining the probability of failure for HTHA of C-1/2Mo equipment.

The first step involves establishing an appropriate value for Pv to characterize the HTHA resistance at the limiting probability of failure level. For example, a risk assessment has determined that the maximum permitted probability of failure for HTHA for the C-1/2Mo equipment being evaluated is a D level as defined by the risk matrix in Figure 1. A description for the C-1/2Mo equipment being evaluated is shown in following table.

C-1/2Mo Pressure Vessel Fabricated from A-204 grade B in the annealed condition and PWHT'd

Operating Period	Timeframe	Years	H_2 Partial Pressure psia (bara)	Temperature °F (°C)
Past	1976-2006	20	200 (13.8)	630 (332)
Future	2006-2026	20	200 (13.8)	665 (352)

At the end of the evaluation the equipment owner wants to know how much life has been consumed to date and whether the vessel will last for another 20 years at the higher operating temperature assuming the C-1/2Mo has HTHA resistance consistent with a D probability of failure. We calculate a Pv value to characterize the HTHA resistance consistent with a D probability level This is done for the specific H_2 partial pressure conditions involved in the assessment. In literature a single Pv value is typically quoted to characterize HTHA resistance. Instead of this approach, we essentially use a position on the Nelson curve to characterize a material's resistance to HTHA and calculate a Pv value based on the position. As a result, we are using the Pv calculation to establish a relative dependence on time at a temperature and hydrogen partial pressure. For establishing the Pv value we use a time of 200,000 hours for the Nelson curve. This is reported in literature[3] as a reasonably conservative time estimate for each of the Nelson curve limits when performing a life assessment. For this example, which is shown in Figure 2, the hydrogen partial level of 200 psia (13.8 bara) intersects the line for a D to C transition (limit for D level probability of failure) at 670°F (355°C). For this type of assessment we have developed a spreadsheet to perform the calculation. The spreadsheet calculation for Pv level shows a result as follows:

Selected Probability Level	**H_2 PP (psia)**	**H_2 PP (kg/cm2)**	**Temperature (°F)**	**Temperature (°K)**	**Pv**
D/E	200.00	14.08	670.00	627.44	4.89

This Pv level of 4.89 which reflects the vessel's resistance to HTHA is used to determine how much HTHA life has been consumed to date and whether all the life will be consumed with an additional 20 years service at more severe operating conditions.

Exposure Time (hrs)	**H_2 PP (psia)**	**H_2 PP (kg/cm2)**	**Temperature (°F)**	**Temperature (°K)**	**Time to Failure (hrs)**	**Life Fraction Consumed**	**Accummulated Life Fraction Consumed**
175200	200.00	14.08	630.00	605.22	1022621	0.17	0.17
175200	200.00	14.08	665.00	624.67	243701	0.72	0.89

This D level assessment indicates that about 17% of the life has been consumed by operation to date, while after another 20 years at the higher temperature operation, a total of almost 90% of the life will be consumed.

VALIDATION OF ASSESSMENT PROCEDURE USING FAILURE DATA EXPERIENCE

This risk based assessment of HTHA of C-1/2Mo was validated against the reported failure experience. The 11 failure experiences closest to the carbon steel curve are shown in Table 1. Each of the failures is plotted in Figure 3 on the Nelson curves for the various assigned probability levels for C-1/2Mo. Each of these 11 were evaluated using the 2 step Pv assessment procedure described in the previous section to determine a calculated remaining life for each reported failure point. The results of this assessment for each failure point in shown in the last 2 columns in Table 1. We performed the assessment for the E to D and D to C demarcation points for the change in probability levels. In effect, these are the limits for the E and D probability levels. For example, for failure point 62 shown in Table 1 we first calculate the Pv value for the transition from the E to D probability level as follows.

Selected Probability Level	H_2 PP (psia)	H_2 PP (kg/cm2)	Temperature (^oF)	Temperature (^oK)	Pv
D/E	190.00	13.38	655.00	619.11	4.82

In step 2, we calculate the life fraction consumed as a function of the listed operating conditions for the failure point.

Exposure Time (hrs)	H_2 PP (psia)	H_2 PP (kg/cm2)	Temperature (^oF)	Temperature (^oK)	Time to Failure (hrs)	Life Fraction Consumed	Accummulated Life Fraction Consumed
191070	190.00	13.38	670.00	627.44	110837	1.72	1.72
1930	190.00	13.38	700.00	644.11	35637	0.05	1.78

For the reported failure point 62, the Pv assessment procedure shows that at a D probability level, the assessment would predict that all the life would consumed. This assessment of failure point 62 indicates that the Pv assessment procedure provides a conservative evaluation HTHA.

The general trends indicated from the results of this evaluation on all 11 reported failure point are the following:

- All 11 failure points shown in Table 1 involved C-0.5Mo in the as-rolled annealed condition. It is recognized that C-0.5Mo possesses much less HTHA resistance in the annealed condition, largely because of the carbides favored in the annealed condition are less resistant to decomposition in the presence of hydrogen. If the C-0.5Mo component is in the normalized or quench and tempered condition, its resistance to HTHA will be significantly better. In recent assessments we have assigned the HTHA resistance of C-0.5Mo steel in the normalized or quench and tempered condition as being half way between the carbon steel curve and the original C-0.5Mo curve. This provides a significantly improved resistance to HTHA and will result in a much lower life fraction consumed using the Pv calculation method. It should be noted that ASTM A-204 requirements for C-0.5Mo plate require that for thicknesses above 1.5-inches the plate must be supplied in the normalized condition.
- The failure data points displaying the worst HTHA resistance are data points 38 and 2. Data point 38 is the only reported failure of C-0.5Mo steel where the welds were not PWHT'd. It is recognized that non-PWHT'd welds are significantly more prone to HTHA. This particular failure involved cracks in the weld HAZ that did not propagate through wall. It appears the welding residual stresses promoted the initiation of HTHA; however, once the residual stresses were relieved by the initial crack formation, the crack did not propagate through wall. This failure data point does highlight the need to pay particular

attention to inspect for cracks at welds on any equipment in HTHA service that is not PWHT'd. Failure data point 2 piping circumferential welds where the root pass was made with a carbon steel filler material. In this situation, the carbon steel would have less resistance compared with C-1/2Mo and initiate a crack that would continue to propagate through the C-1/2Mo. In this particular failure case, the it was also uncertain how effectively the circumferential weld seams were PWHT'd.

- The next worst reported failure point was 62. In this case, only surface blistering and no significant through wall cracking below the surface blisters were reported. This type of blistering is commonly referred to as "methane blistering" because it is caused by methane build up at laminations in the steel from the decomposition of carbides in close proximity to the laminations. This has been observed in both C-0.5Mo and 1 1/4Cr steels well below the Nelson Curve limits in Figure 1 of API RP-941[4]. Methane blistering is mainly associated with impurity levels in the steel and its propensity to form laminations and create locations where methane can collect and build up. In general, we do not feel "methane blistering" results in the same level of damage as through wall fissuring generated by internal HTHA. For this same reason, the API HTHA task group has not used reports of "methane blistering" to move the Nelson Curve.
- Failure data points 45 and 46 both show a calculated life fraction consumed at 0.9 at the D/C probability demarcation point. Having 2 reported failure points with calculated life fractions slightly below 1.0 for this probability level would appear reasonable considering all of the reported incidents of HTHA of C-0.5Mo and considering the amount of C-0.5Mo equipment in HTHA service worldwide, This also appears consistent with the qualitative definitions for both the C and D probability levels. It should also be noted that some of our refinery locations have used 0.8 life fraction consumed at the assessment probability level as the point where life is consumed. This is a more conservative approach with added safety margin.

This review of the failure data supports our qualitative risk based procedure for setting a probability of failure associated with HTHA. This includes the use of the Pv calculation for life fraction consumed to take into account the time at temperature and hydrogen partial pressure. This failure data also indicates that if a location wants to be more conservative, it can include an additional safety margin by reducing the allowed life fraction consumed from 1.0 to 0.8.

INSPECTION REQUIREMENTS FOR EQUIPMENT IN HTHA SERVICE

Our current Company practice is to perform an inspection for HTHA once the calculated life fraction as defined by the Pv calculation procedure described in this paper reaches 0.8 to 1.0. We have a defined inspection procedure for HTHA that involves ultrasonic back scatter and other ultrasonic techniques for detecting HTHA. If no HTHA damage is found after an inspection is performed, we typically permit continue service, but require a re-inspection for HTHA after an additional incremental 10% of the life is consumed using the risk based Pv calculation procedure.

We established this 10% incremental life consumed threshold for re-inspection based on our experience detecting HTHA using ultrasonic inspection techniques. We expect that our defined ultrasonic inspection procedure for HTHA can only detect HTHA damage once fissures form in the metal. It is not expected that the prescribed ultrasonic techniques will detect methane bubbles and other damage expected early in life in high temperature high pressure hydrogen service. Also, our experience indicates that internal fissuring from HTHA is not expected until late in the life of the equipment after about 90% of the life has been consumed.

This current basis for re-inspecting equipment in HTHA is the single most restrictive requirement for equipment operating at conditions where the equipment is considered susceptible. Frequently, the 10% incremental life consumed for an acceptable probability level is significantly less than the run length between planned turnarounds. In specific situations we have developed and qualified ultrasonic procedures for detecting HTHA for use on equipment at operating temperatures. In any event, this re-inspection requirement after an additional 10% incremental life consumed remains the single most difficult requirement in managing C-1/2Mo equipment operating in a vulnerable HTHA range.

CONCLUSIONS

1. A qualitative risk based assessment procedure has been developed based on the requirements of the ExxonMobil risk matrix to assess the vulnerability of C-1/2Mo equipment to HTHA. This procedure determines the probability of failure based on the relative position on the Nelson curve and the HTHA dependence on time at temperature and hydrogen partial pressure as captured by the Pv relationship.
2. This assessment procedure was validated using an assessment of 11 reported C-1/2Mo HTHA failures closest to the carbon steel curve. This includes 9 failures reported to the API and 2 failures experienced at ExxonMobil facilities not reported to API. This assessment indicated that the probability setting guidance provided in the risk based evaluation procedure was reasonable.
3. Our present inspection procedures involve the use of ultrasonic back scatter and other techniques capable of detecting internal fissuring typically associated with the advanced stages of HTHA. Re-inspection is required after an additional 10% incremental life is consumed. This re-inspection requirement remains the single most difficult requirement in managing C-1/2Mo equipment operating in a vulnerable HTHA range.

REFERENCES

1. Merrick, R.D. and Ciuffreda, A.R., Proceedings - Refining Division 47th API Midyear Meeting, May, 1982, vol. 61, page 101
2. Sundararajan, G. and Shewmon, P.G., Metall. Trans. A, 1980, vol. 11A, p. 509
3. Saugerud, O.T., Moore, D.E. and Odette, R.G., "A Model-Based Approach to Evaluating the Probability and Criticality of Hot Hydrogen Attack in C-1/2Mo Equipment", Proceedings from the 1992 ASME PVP Meeting, PVP-Vol. 239/MPC-Vol. 33, Servieability of Petroleum, Process and Power Equipment, ASME 1992
4. Merrick, R.D. and Maguire, C.J., "Methane Blistering of Equipment in High Temperature Service", Paper No. 30, Presented at the Annual Meeting of the National Association of Corrosion Engineers, March, 1979.

Table 1: Data Summary and Pv Calculations for 11 HTHA Failures Closest to the Carbon Steel Nelson Curve

Data Point	Temperature °F (°C)	H_2PP psia (bara)	Time to failure (hours)	Description of Equipment and Condition of C-0.5Mo Steel	Life Fraction Consumed (D/E line)	Life Fraction Consumed (C/D line)
62	670 (354) ave 700 (371) max	190 (13.1)	193,000	A-204 grade B plate, assumed in as-rolled condition, naphtha hydrotreater service, cracks in weld HAZ, no report of leak, only surface blistering observed, welds were PWHT'd	1.78	0.67
39	698 (370) ave 752 (400) max	285-300 (19.7-20.7)	96,250 at ave. 8750 at max	A-335 pipe, assumed in as-rolled condition, cracks observed in weld HAZ, piping was PWHT'd	18.32	7.13
43	625 (329) ave 675 (357) max	350 (24.1)	151,200	A-204 grade B as rolled plate, PWHT'd at 1100 °F	6.00	1.87
46	626 (330) ave 680 (361) max	350 (24.1)	131,250	Welded piping from 0.55-inch thick A-204 grade B plate in as rolled condition, PWHT'd condition, crack in seam weld HAZ	3.06	0.90
45	620 (327) ave 640 (338) max	457 (31.5)	78,750	1.2-inch thick A-204 grade B plate in as rolled condition, PWHT'd after welding	3.83	0.91
51	690 (366) ave 725 (385) max*	397 (27.4) ave 500 (34.5)max*	175,000	A-204 grade C Hx tubesheet, basemetal cracking, no information on heat treatment condition	59.43	1.23
38	620 (327) ave 675 (357) max	270 (18.6)	83,000	A-335 piping in as rolled condition and not PWHT'd, cracking observed but piping did not leak	0.55	0.13
63	600 (316) ave 750 (399) max	500 (34.5)	233,000	A-204 grade C plate with Type 405 cladding, 1180 °F PWHT	15.45	4.89
64	600 (316) ave 770 (410) max	525 (36.2)	281,000 ave 1920 max	A-204 grade C plate with Type 405 cladding, 1170 °F PWHT	26.54	10.34
1	608 (320)	181 (12.5)	210240	Seamless C-1/2Mo piping, HTHA initiated in root pass of circ weld which was made with carbon steel consumable. Uncertain about PWHT conditions	0.17	0.05
2	788 (420)	174 (12)	254040	C-1/2Mo heater tube HAZ at weld between C-1/2Mo and 1 1/4Cr section. Uncertain about PWHT condition	145.1	49.9

* 1 to 2% of the operating time

Figure 1: ExxonMobil Risk Matrix

CONSEQUENCE	PROBABILITY A	B	C	D	E
I					
II					
III					
IV					

PROBABILITY CATEGORY	DEFINITION
A	Possibility of repeated incidents => **Very Likely**
B	Possibility of isolated incidents => **Somewhat Likely**
C	Possibility of occurring sometime => **Unlikely**
D	Not likely to occur => **Very Unlikely**
E	Practically impossible => **Practically Impossible**

<u>**Figure 2: C-1/2Mo HTHA Curves Defining the Associated Probability of Failure**</u>

Probability Settings for HTHA of C-1/2Mo

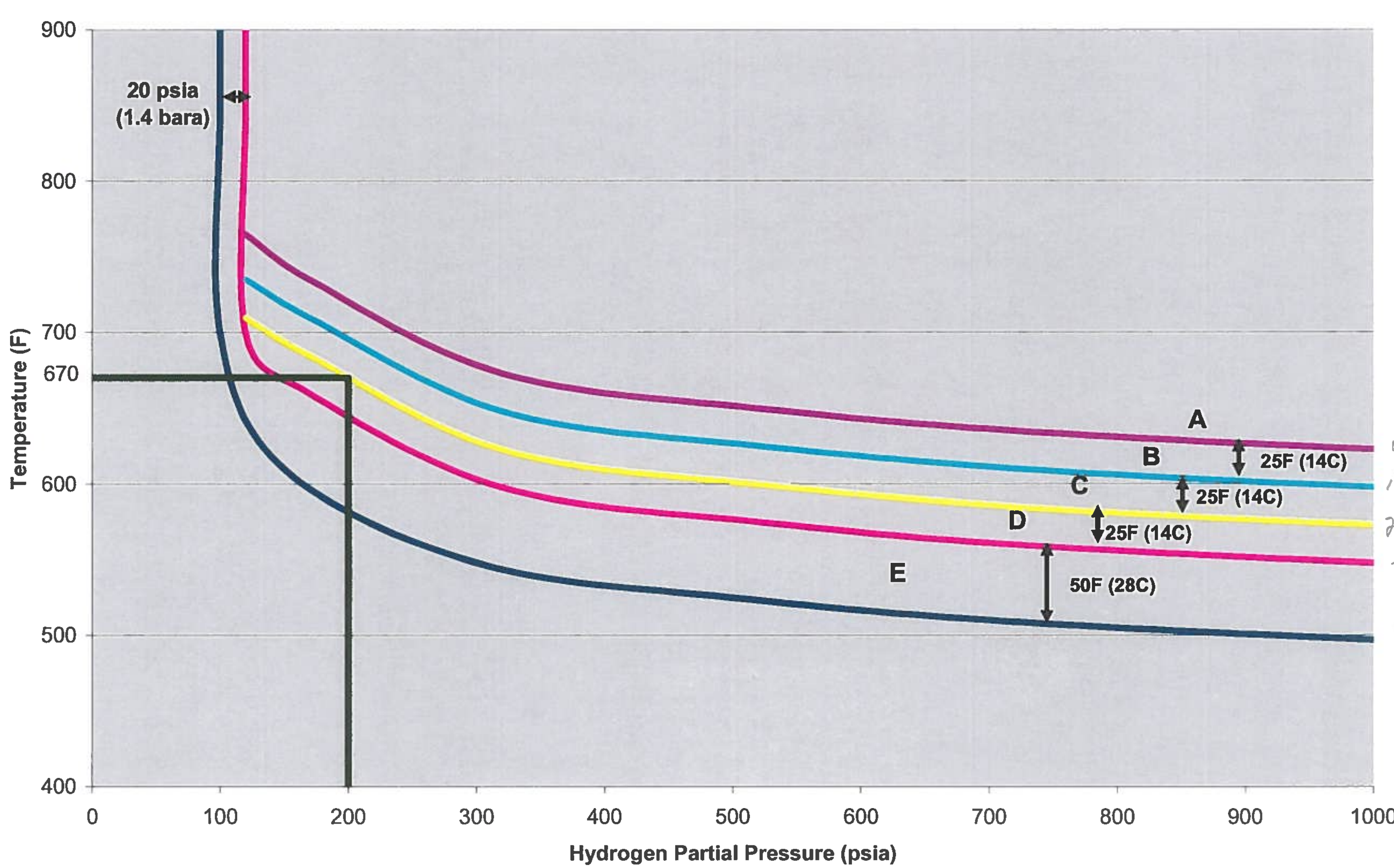

125 °F 70 °C
100 56
75 42
— Effective

Figure 3: C-1/2Mo HTHA Curves with the 11 Reported Failures Closest to the Carbon Steel Nelson

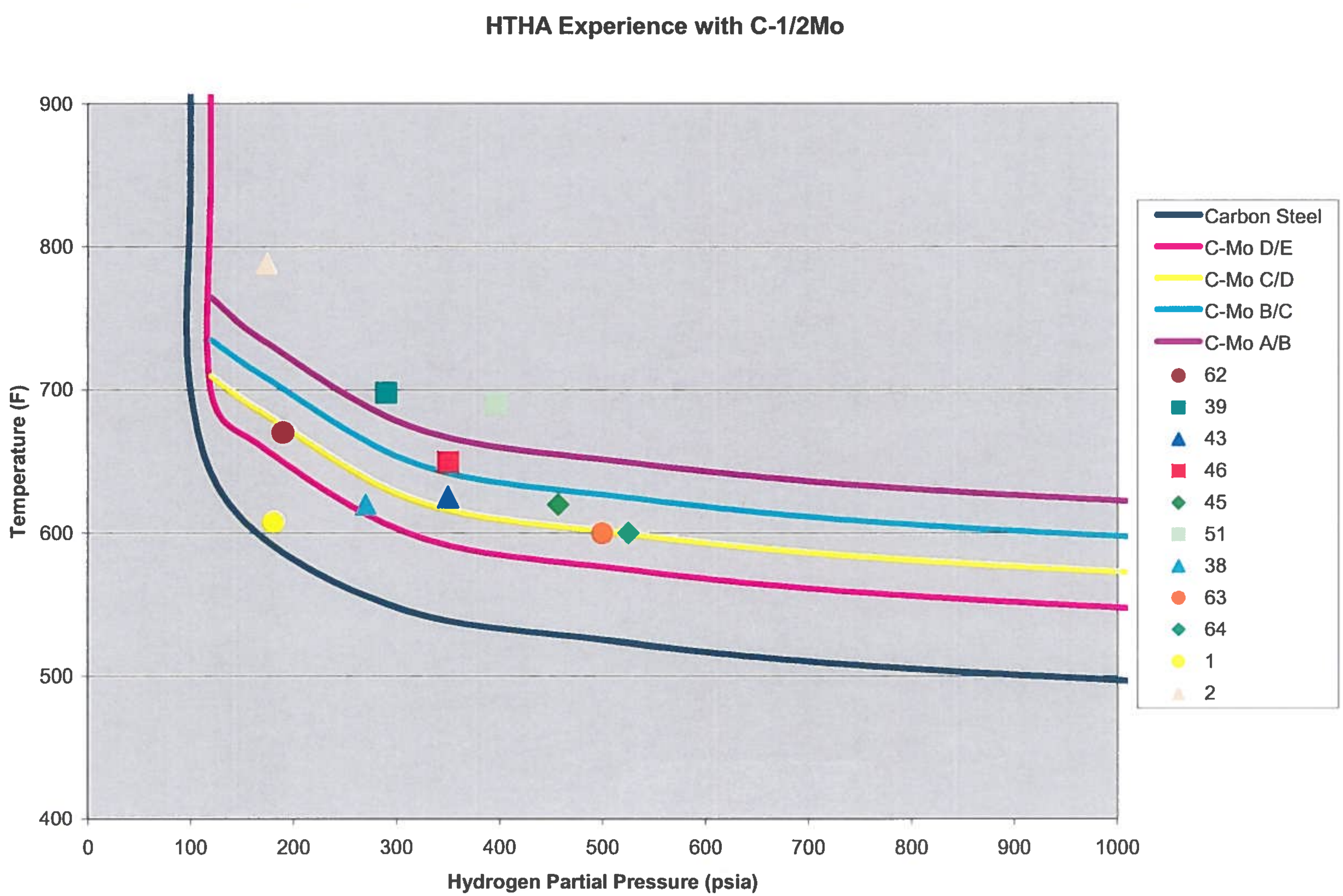

Proceedings of 2010 ASME Pressure Vessels and Piping Conference
July 18-22, 2010, Bellevue, Washington

PVP2010-25455

Cracking of non-PWHT'd Carbon Steel Operating at Conditions Immediately Below the Nelson Curve

James McLaughlin
Joseph Krynicki
Thomas Bruno
ExxonMobil Research and Engineering Company
Fairfax, VA

ABSTRACT

Cracking was observed in non-PWHT'd carbon steel piping and vessels operating at conditions immediately below the "Nelson" curve. This curve provides a threshold limit for high temperature hydrogen attack as a function of the equipment operating temperature and hydrogen partial pressure. This curve is based on industry experience with steel equipment operating for many years in high temperature high pressure hydrogen service. Our investigation indicated that cracking occurred in 2 stages. Stage 1 or the initial stage of cracking appeared to occur as a result of intergranular "hydrogen assisted" cracking very similar to high temperature hydrogen attack. It appears that Stage 1 cracking is driven by the combined effects of residual welding stresses and "methane pressure" stresses from the decomposition of carbides. The circumstances of the observed cracking indicate that, unlike high temperature hydrogen attack, it occurred over a relatively short period of time after an operating change to a higher hydrogen partial pressure. Stage 2 cracking results from sulfide scale packing the crack during high temperature operation in a sulfidizing environment and causes the Stage 1 cracks to further propagate through wall. Once the sulfide scale filled crack cools down during a shutdown, the surrounding metal contracts around the scale and causes a high load on the crack tip which promotes further crack propagation. The presence of dissolved hydrogen in the steel further promotes Stage 2 crack propagation during shutdown periods.

INTRODUCTION

Cracking of carbon steel piping and vessels occurred in hydrotreating service operating at temperatures between 550 and 600°F (288 and 316°C) and hydrogen partial pressures between 100 and 200 psia (6.9 to 13.8 bar). In each case cracking occurred at welds that were not subjected to post weld heat treated (PWHT'd). Cracking was observed in bare carbon steel reactor vessels and heat exchanger channel sections, and carbon steel effluent piping in light distillate hydrotreating units. The locations in these units where cracking has been observed are illustrated in the simplified process flow diagram shown in Figure 1. All of the observed cracking originated at the ID surface. In each case cracking was initially discovered by an onstream leak. Upon shutdown of the equipment, additional inspection uncovered additional cracking at welds. For vessels, cracking was observed at both longitudinal and circumferential weld seams. These units only had seamless piping, and all cracking was observed at circumferential butt welds.

Laboratory Examination of Cracked Weld Samples

Samples from both cracked vessel welds and cracked piping welds were examined in the laboratory. The examined cracked piping was fabricated from ASTM A-106 grade B, while the examined cracked vessel was fabricated from ASTM A-515 grade 70. Figure 2 shows cross sections through typical cracks observed in vessel and piping welds. The typical piping sample crack occurred in the weld base metal material in an area close to the weld where residual welding stresses are expected to be highest. The typical vessel sample cracked in the coarse grain heat affected zone (HAZ) of the weld close to the weld fusion line. Welding residual stresses are not expected to be highest in this area of the weldment; however, the coarse grain HAZ generally does have inferior properties and is more susceptible to environmental and creep cracking.

As illustrated at higher magnification in Figure 3, cracks from pipe samples close to the ID surface were filled with scale. A cracked pipe sample was broken open to expose the fracture surface. As shown in Figure 4 the fracture surface is entirely intergranular and covered with FeS scale. As illustrated in Figure 5, the observed cracking in pipe samples close to the OD surface typically contained less scale or no scale at all.

Examination at higher magnification of cracks near the ID surface on plate samples from the reactor vessel displayed intergranular fissures that were associated with pearlite colonies. This is illustrated in the scanning electron microscope photos shown in Figure 6. It also appears that the cementite (Fe_3C) carbide has experienced some degradation which is typically associated with fissuring caused by high temperature hydrogen attack (HTHA).

Conclusions from Laboratory Examination of Cracked Piping and Vessel Samples

We concluded from our laboratory examination of the cracked piping and vessel samples that cracking occurred in 2 stages.

Stage 1 Cracking

Cracking appears to have initiated at the ID surface as a result of the combined effects of residual welding stresses and pressure stresses generated at grain boundaries by methane formation from the degradation of the cementite (Fe_3C) carbides found in carbon steel. Pressure stresses generated by methane formation are driven by the carbide degradation as shown by the following equilibrium between hydrogen, the carbide and methane.

$$\mathbf{MC + 2H_2 <=> CH_4 + M \ (1)}$$

The methane pressure generated by this equilibrium with cementite is enormous as illustrated in Table 1.[1] This table shows equilibrium methane pressures that can be generated at temperatures and hydrogen partial pressures close to, but just below, Nelson curve conditions. It should be noted that these equilibrium pressures are probably not achieved, due to a combination of several kinetic limitations such as limitations on the amount of methane generated at a grain boundary due to carbon mobility at these moderate temperatures, and, grain boundary fissuring before reaching the equilibrium pressure.

The general appearance of the fissuring associated with Stage 1 cracking as illustrated in Figure 6 suggests that this cracking may be generated in part by the same methane pressures that drives HTHA. However, the general appearance of the fissures shown in Figure 6 suggests that Stage 1 cracking is not associated with the same time dependent creep mechanism generally associated with HTHA. A comparison between the fissures characteristic for Stage 1 cracking with the methane bubbles associated with the initial stages of "typical" HTHA suggest that Stage 1 cracking may share a common driving force in methane pressure, but not the same time dependent creep mechanism. Figure 7 compares the grain boundary fissuring characteristic for Stage 1 cracking with the initial stages of conventional HTHA[2] which displays methane bubbles at grain boundaries.

Our conclusion that Stage 1 cracking takes place over a shorter period of time compared with HTHA suggests that Stage 1 cracking is most likely associated with a change in operating conditions that leads to a higher methane pressure stress that initiates the cracking. An evaluation of recent operating conditions for the process unit that experienced the observed cracking in piping and vessels in relation to the carbon steel Nelson curve is shown in Figure 8. Our analysis of the process data shows that over a 3 year period this unit operated at higher hydrogen partial pressure levels in the range of 90 to 200 psia (6.2 to 13.8 bar),compared with the historical hydrogen partial pressure range of 60 to 70 psia (4.1 to 4.8 bar). The range of operating conditions experienced during this period of operating at a higher hydrogen partial pressure is shown by the yellow data points, while the historical operating range is illustrated by the green box. As shown in Table 1, in this temperature range (500°F (260°C) to 600°F (316°C)), the equilibrium methane pressure at a hydrogen partial pressure of 200 psia (13.8 bara) is approximately 10 times higher than the equilibrium methane pressure generated at 60 psia (4.1 bara). This suggests that the Stage 1 cracking occurred during the operating period when the hydrogen partial pressure was significantly higher.

Stage 2 Cracking

Once Stage 1 cracking occurs the residual welding stresses that promoted cracking will relax. Once the residual welding stresses relax, we believe Stage 1 crack propagation stops. The laboratory examination of cracking indicates that cracking near the OD surface of the piping and vessel samples display less sulfide scale and in some cases no scale at all for cracks closest to the OD surface. This suggests that crack propagation continued as a result of sulfide scale formation in cracks open to the ID surface from exposure during operation in a high temperature sulfidizing environment. Upon shutdown of the equipment and cooling to ambient temperature, the sulfide scale in the cracks will contract less than the surrounding metal imposing a "wedge opening" tensile load on the crack tip. Crack propagation will occur until the "wedge opening" load is relaxed. It should also be noted that crack propagation during a shutdown and cooldown to an ambient temperature will be promoted by the dissolved hydrogen remaining from operation at an elevated temperature at a significant hydrogen partial pressure. It is well known that dissolved hydrogen in steel reduces the crack-tip stress intensity at which a crack will propagate.

It is difficult to determine precisely how much of the through wall cracking for the piping and the vessels can be attributed to Stage 1 or 2 cracking. In the earlier discussion of an example of observed cracking, it was hypothesized that Stage 1 cracking occurred as a result of operation for three years at a higher hydrogen partial pressure. This three year operating period ended four years before a through wall leak was noticed. During this four year period, the unit experienced two shutdowns or cycles when Stage 2 crack propagation would be possible. Also, our experience with crack propagation at shutdowns related to sulfide scale formation in a crack, suggests that only a relatively small amount of crack propagation occurs during each shutdown cycle.[3] As a result, we conclude that most of the through wall crack propagation, leading to the observed leaks, occurred as Stage 1 cracking.

Other Contributing Factors to Cracking

Up to this point, this paper has only discussed two common characteristics for the observed cracking at welds in carbon steel equipment. These characteristics are carbon steel that is not subjected to PWHT'd after welding and equipment that is operated at conditions close to but just below the Nelson curve limits for carbon steel. We would expect that these two factors play a role in dictating the tendencies and extent of Stage 1 cracking. We would expect that these two factors would not play a role in Stage 2 crack propagation. Stage 2 cracking is primarily dictated by the presence of a sulfide scale in the cracks. It is expected that all carbon steel equipment in hydrotreating service would be susceptible to forming a sulfide scale in cracks open to the ID surface due to the sulfidizing process conditions.

We would expect that these other contributing factors to cracking, as discussed in this section of the paper, would be primarily associated with Stage 1 cracking. Our experience with the observed cracking and follow-up inspections of other non-stressed relieved carbon steel equipment in similar service suggest that two other factors may contribute to the severity of Stage 1 cracking. The two factors are steel cleanliness/microstructure and strength level of the steel. The vessel with cracks we examined was fabricated from an early 1970's vintage carbon steel with a coarse grain size (ASTM A-515 grade 70). The combination of a coarse grain size and higher impurity levels will tend to reduce grain boundary strength and under equivalent operating conditions make it more susceptible to Stage 1 cracking. The experience we have with the vessel that cracked and leaked needs to be compared with a second vessel in identical service in the same unit. This vessel, which was added to the unit later as part of a de-bottlenecking project, was erected in the mid-80's and is fabricated from a more recent vintage steel (ASTM A-516 grade 60). This vessel did not leak; however, a recent inspection of welds on this vessel did find cracks growing from the ID surface. We expect that this vessel also experienced Stage 1 cracking, but to a lesser extent (in terms of crack depth and number) compared to the vessel that leaked.

The second consideration or factor that may affect the tendency and extent of Stage 1 cracking is steel strength level. The steel strength level will drive the level of residual welding stresses that can be achieved when welding without PWHT. The higher strength grade 70 steel is expected to have higher residual welding stresses than the lower strength grade 60 steel.

Recommendations to Find/Mitigate Cracking

As a result of finding cracks in non-PWHT'd carbon steel equipment operating at conditions immediately below the Nelson curve, we have established inspection recommendations based on the equipment's operating conditions. If non-PWHT'd carbon steel equipment operates in the temperature and hydrogen partial pressure conditions illustrated by the area marked in red in Figure 9, an inspection of welds for cracking is recommended. The inspection guidance for any specific situation depends on the associated risks. Our suggested approach, which calls for different levels of inspection coverage (% of welds) and inspection methods, is based on the severity of the service. A summary of our tiered inspection approach includes:

High Level of Inspection Effectiveness

- Automated shear wave UT(SWUT) or TOFD (time of flight diffraction) inspection of all welds

Medium Level of Inspection Effectiveness

- Automated shear wave UT(SWUT) or TOFD (time of flight diffraction) inspection of a significant portion of the welds

Standard Level of Inspection Effectiveness

- Manual or automated SWUT, or, TOFD. Scope to be determined in accordance with method.
- RT with specific considerations for equipment application (e.g. pipe size), inspection performance (e.g. image quality), and re-inspection interval.

We also provide suggested guidance on when to re-inspect equipment that operates at the conditions illustrated in Figure 9. Since our investigation into this cracking mechanism indicates that it is primarily dependent on hydrogen partial pressure, we believe that if an inspection indicates that the equipment is crack-free, and if we can demonstrate through processing monitoring that the equipment does not operate at more severe hydrogen partial pressure conditions in the future, then there is no need to perform another inspection in the future for this particular mode of failure. We have defined the hydrogen partial level as follows for evaluating whether more severe conditions exist and there is a need for a re-inspection of the equipment.

1. The past operating hydrogen partial pressure must first be evaluated. We recommend using 24-hour average hydrogen partial pressure for the past 5-years operation of the equipment from the time the inspection was performed. Based on this hydrogen partial pressure data one can determine the highest 1-month (30 day) rolling average hydrogen partial pressure level for the entire past 5-year period.
2. A re-inspection of the equipment for this particular mode of cracking is not required as long as the future 1-month (30 day) rolling average hydrogen partial pressure level does not exceed the highest 1-month (30 day) rolling average hydrogen partial pressure for the 5-year period prior to the initial inspection where no cracking was observed.

It should be noted that evaluating hydrogen partial pressure levels going back for a period of 5-years to determine the highest 1-month rolling average prior to the initial inspection was somewhat arbitrary. This 5-year period was based on how far back we would expect each refinery could retrieve operating data. A refinery may have operating data that extends back even further in time. This may show periods where the hydrogen partial pressure was even higher and provide a higher hydrogen partial pressure threshold for requiring the need for re-inspection in the future.

Conclusions

The conclusions from our investigation of cracking of non-stress relieved carbon steel vessels and piping operating close to but immediately below the Nelson curve include the following:

1. Our laboratory examination indicates that cracking occurs in two stages. Stage 1 involves cracks that initiate as fissures along grain boundaries as a result of the combined effects of residual welding stresses and methane pressure. Decomposition of the cementite carbide that is present in carbon steel generates the methane pressure. Stage 2 involves further propagation of Stage 1 cracks. This occurs as a result of sulfide scale corrosion product filling the cracks during operation and subsequently causing "wedge opening" loading during cooldown at shutdown.
2. Examination of the fissures at crack initiation points indicates that this form of cracking is different than conventional high temperature hydrogen attack (HTHA). This cracking initiates as grain boundary fissures as compared with conventional HTHA which initiates as methane bubbles (microvoids) along grain boundaries.
3. Our metallurgical analysis of field collected samples has lead us to conclude that this form of cracking is not time dependent, but rather, condition dependent. Based on the literature that discusses the equilibrium methane pressures resulting from carbide decomposition as a function of temperature and hydrogen partial pressure, we concluded that cracking tendencies depend primarily on hydrogen partial pressure levels - the higher the hydrogen partial pressure level, the higher the likelihood of cracking.
4. Other factors such as steel impurity levels and strength also may play role in determining cracking tendencies, but these factors will be secondary to the service exposure as indicated by the hydrogen partial pressure level for the service.
5. Inspection guidance was developed for all non-stress relieved carbon steel equipment in the operating range reflected in Figure 9. We also provide guidance on how to determine if a re-inspection is needed once an inspection has been performed and no cracking is found.

REFERENCES

1. Shewmon, P.G., Metallurgical Transactions A, 1976, vol. 7A, p. 279
2. The Technical Basis Document for API RP 941, API Technical Report 941, September 2008
3. Adams, N.J.I. and Welland, W.G., 5 International Conference on Pressure Vessel Technology, p. 777, San Francisco, 1985

Table 1: Calculated equilibrium methane pressures generated from degradation of cementite as shown by equation 1.

Temperature (°F)	Temperature (°C)	H_2 Partial Pressure (psia)	H_2 Partial Pressure (atm)	Equilibrium CH_4 Pressure (ksi)
500	260	60	4.08	4996
500	260	100	6.80	14544
500	260	200	13.61	58176
550	288	60	4.08	1926
550	288	100	6.80	5658
550	288	200	13.61	22633
600	316	60	4.08	743
600	316	100	6.80	2201
600	316	200	13.61	8805

Figure 1: Areas in a light distillate hydrotreating unit where cracking of non-PWHT'd carbon has occurred

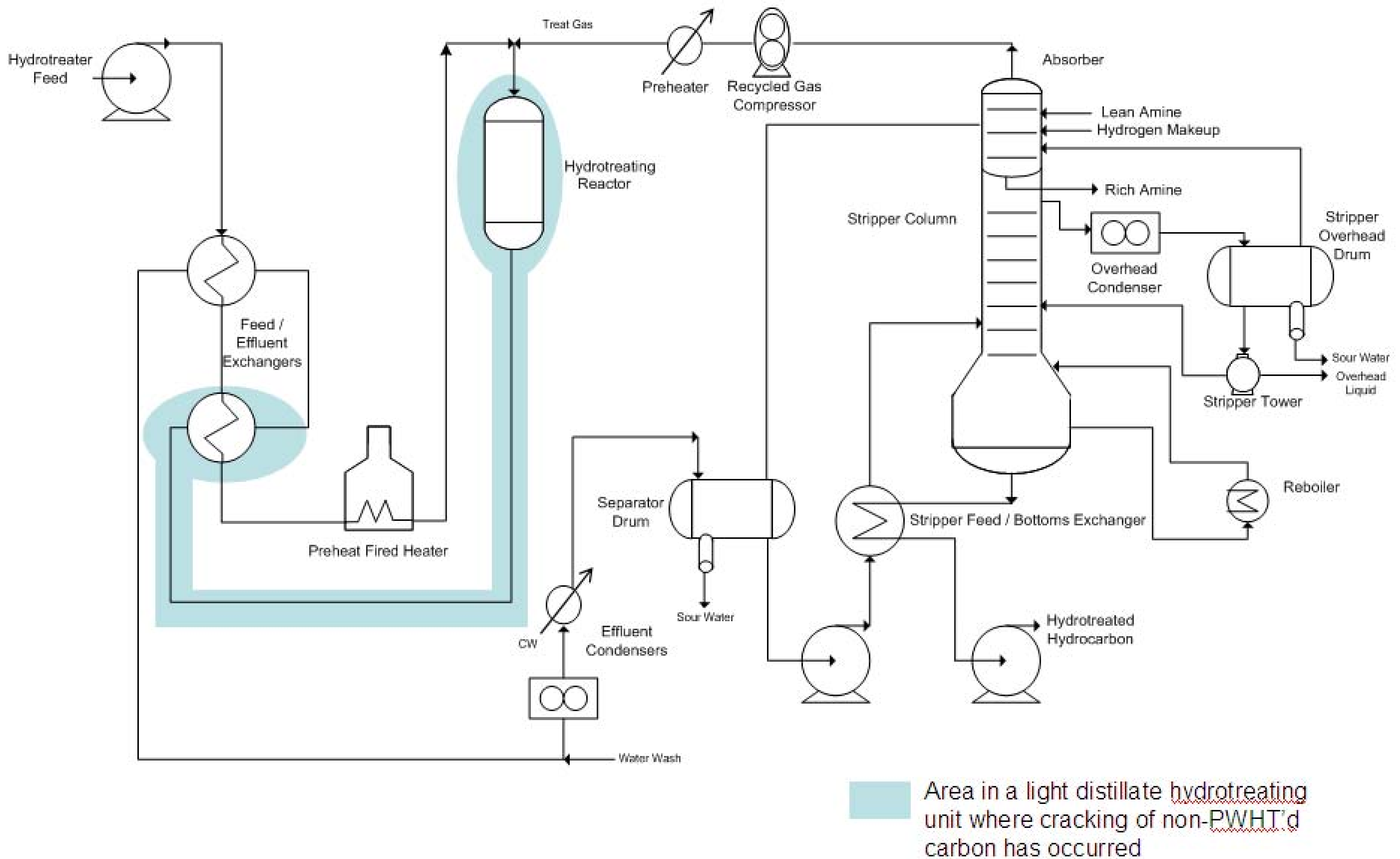

Figure 2: Typical cross-sectional views of cracking observed in vessel and piping welds

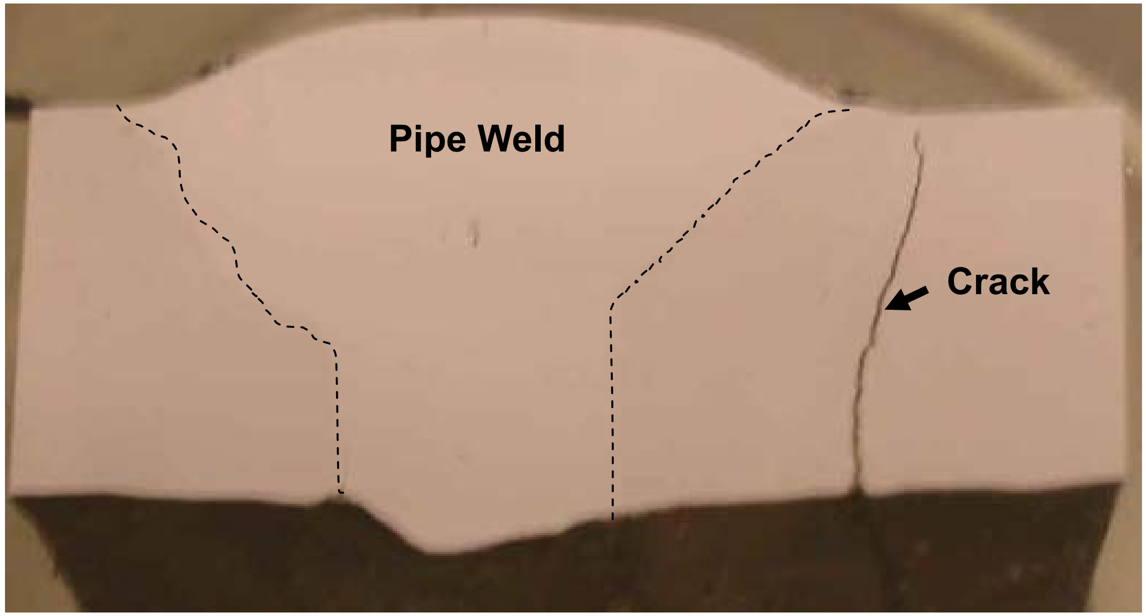

3X

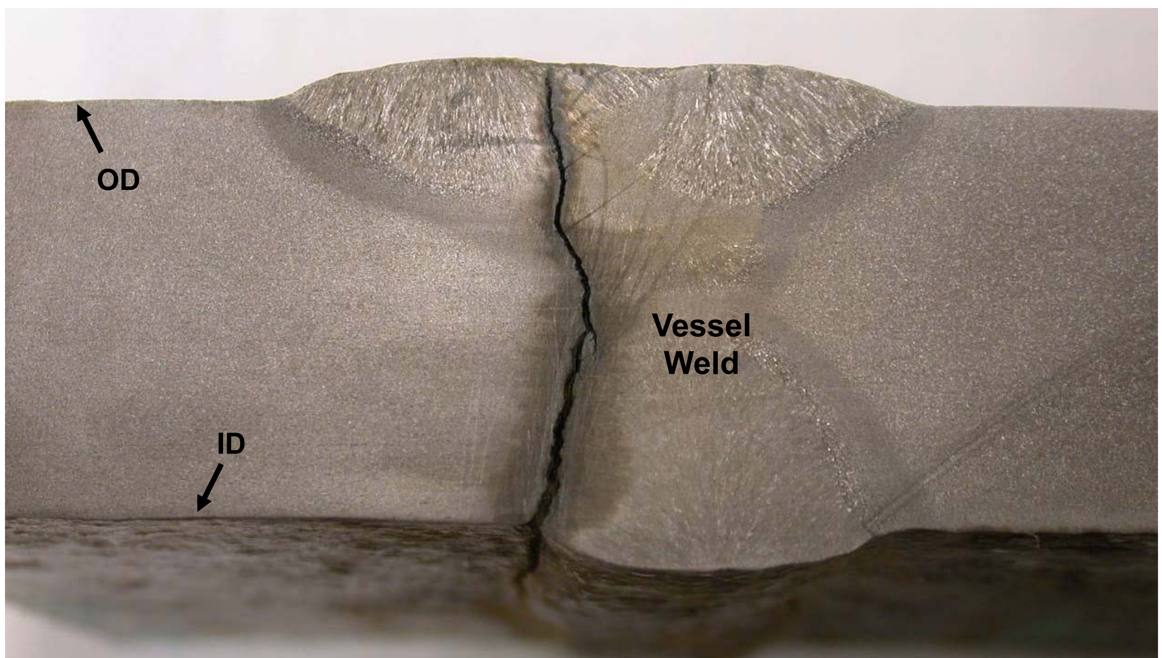

3X

Figure 3: At higher magnification cracking found in piping weldments were filled with scale, especially in areas close to the ID surface

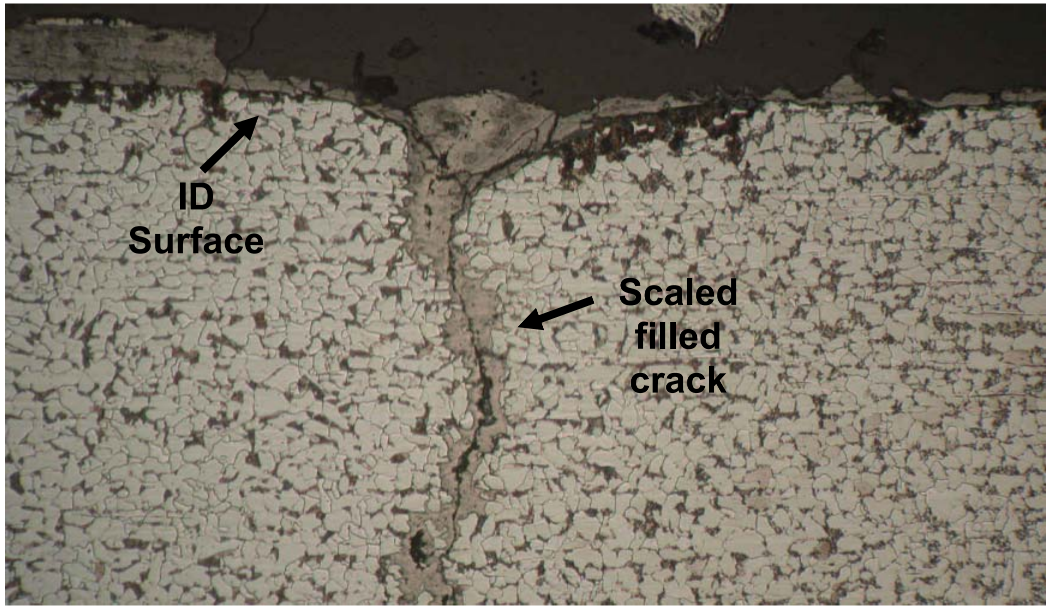

50X

Figure 4: Examination of a crack surface from a piping sample shows it is entirely intergranular and covered with FeS scale.

Intergranular fracture surface covered with FeS scale

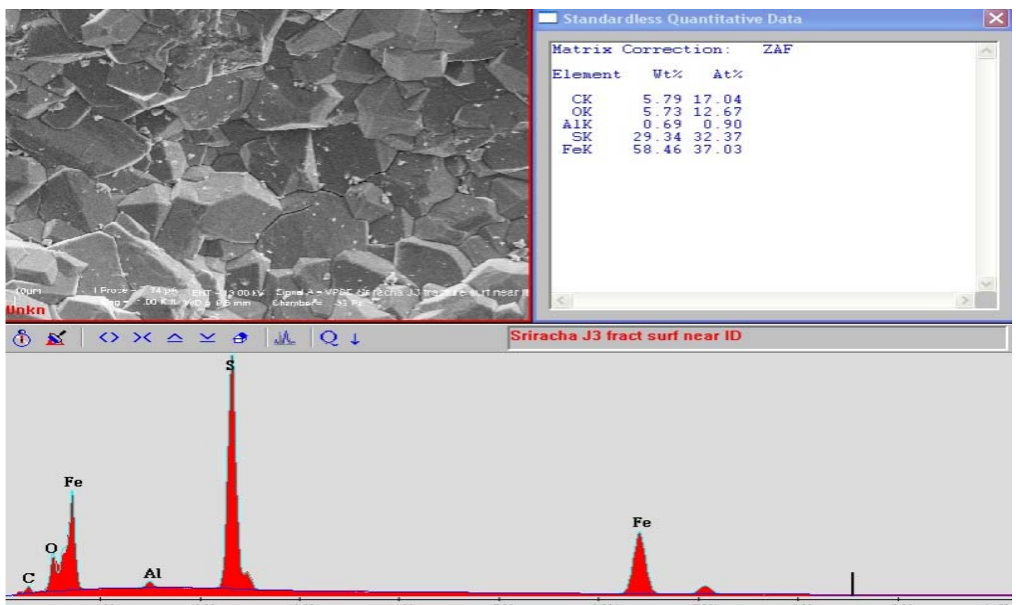

Figure 5: Cracks in a pipe sample near the OD surface contained less scale and in some cases no scale at all.

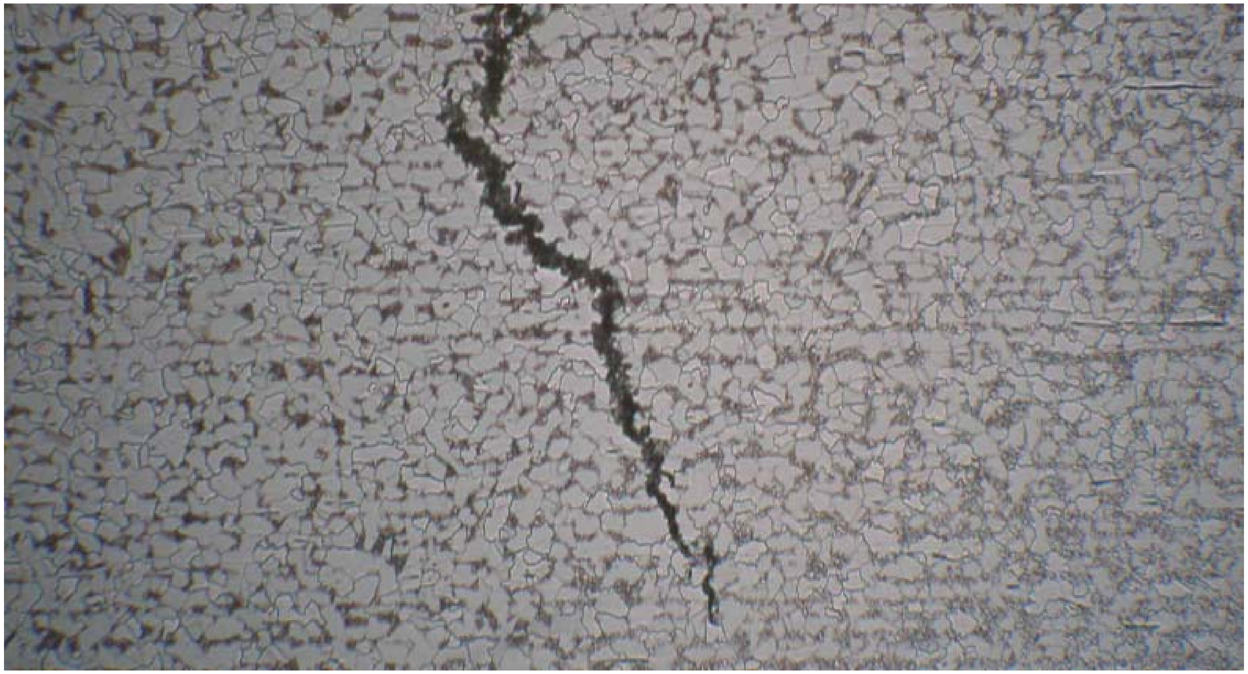

100x

Figure 6: At higher magnification intergranular fissures next to pearlite colonies were observed.

2500x

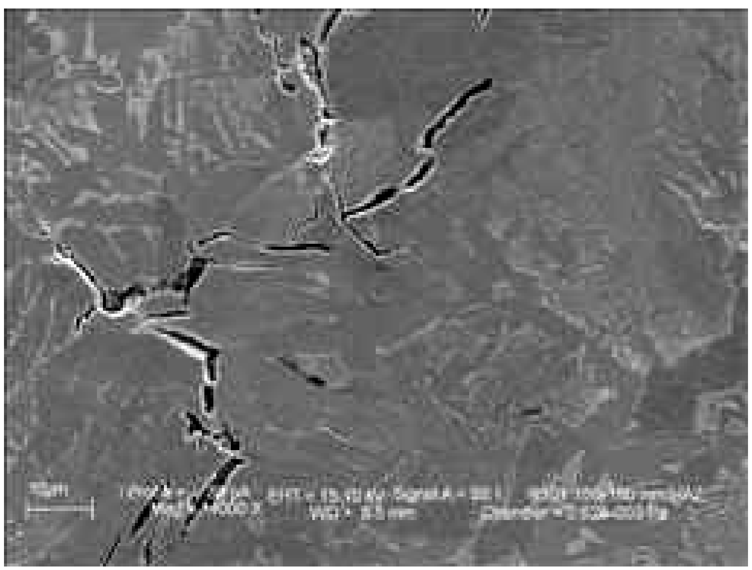

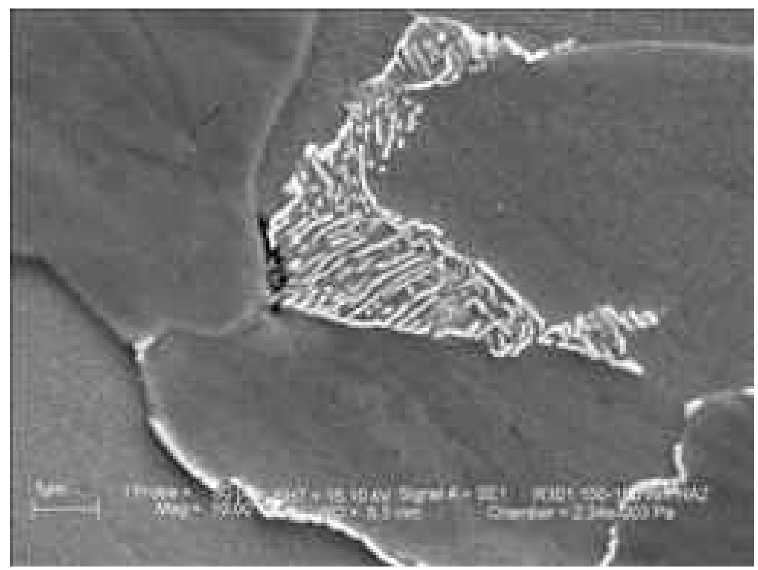

5000x

Figure 7: The fissuring observed with Stage 1 cracking was distinctly different than the methane bubbles observed during the initial stages of HTHA

Comparison of 1st stage cracking with high temperature hydrogen attack suggests 1st stage cracking may not be time dependent but solely dependent on hydrogen partial pressure

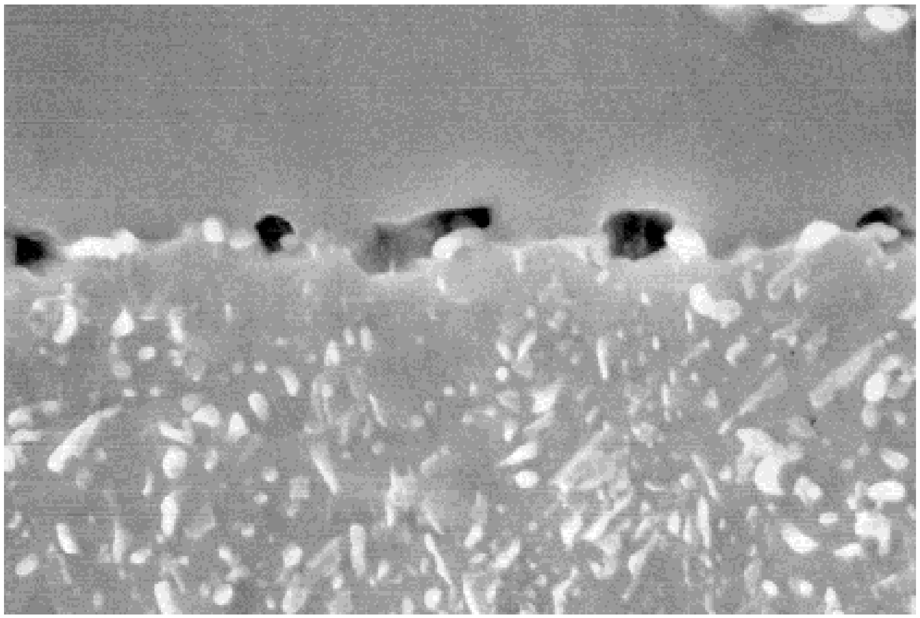

Conventional HTHA - methane bubbles as expected at elevated temperatures due to time dependent creep (Ref. 2)

10000x

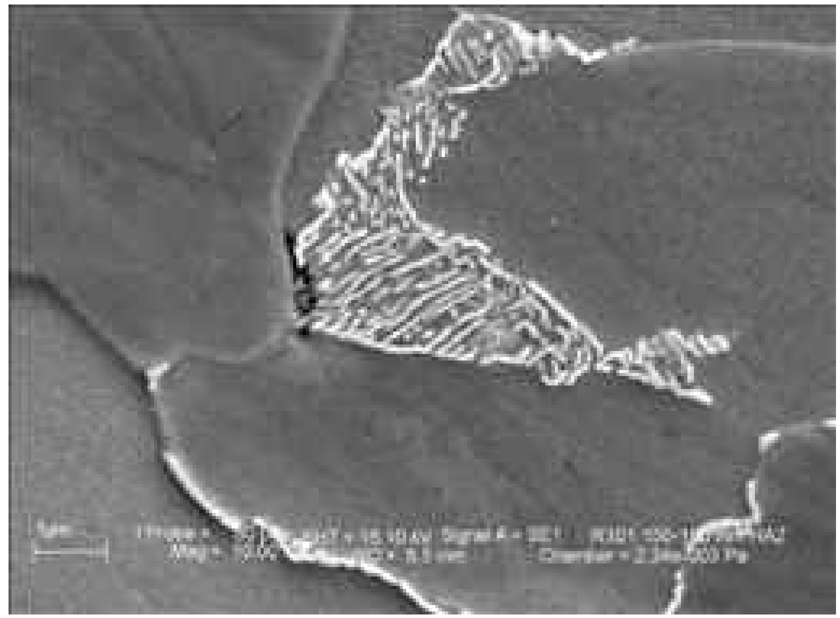

Stage 1 cracking – fissures but no bubbles suggesting that time dependent creep is not occurring

5000x

Figure 8: Unit operating conditions when the hydrogen partial pressure was significantly higher than historical levels.

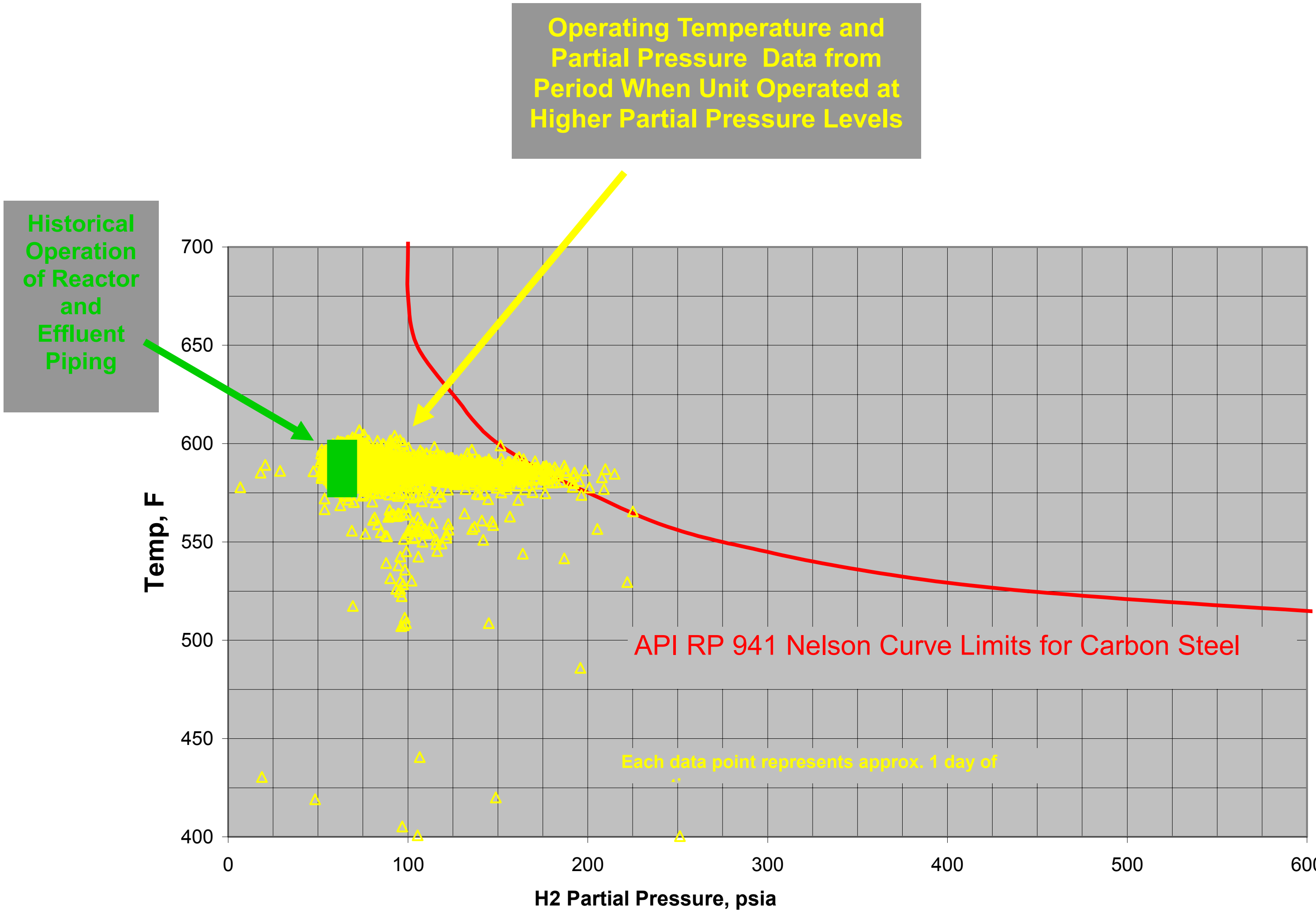

Figure 9: Inspection for cracks is recommended for non-PWHT'd carbon steel vessels that operate at conditions illustrated by the area highlighted in red.

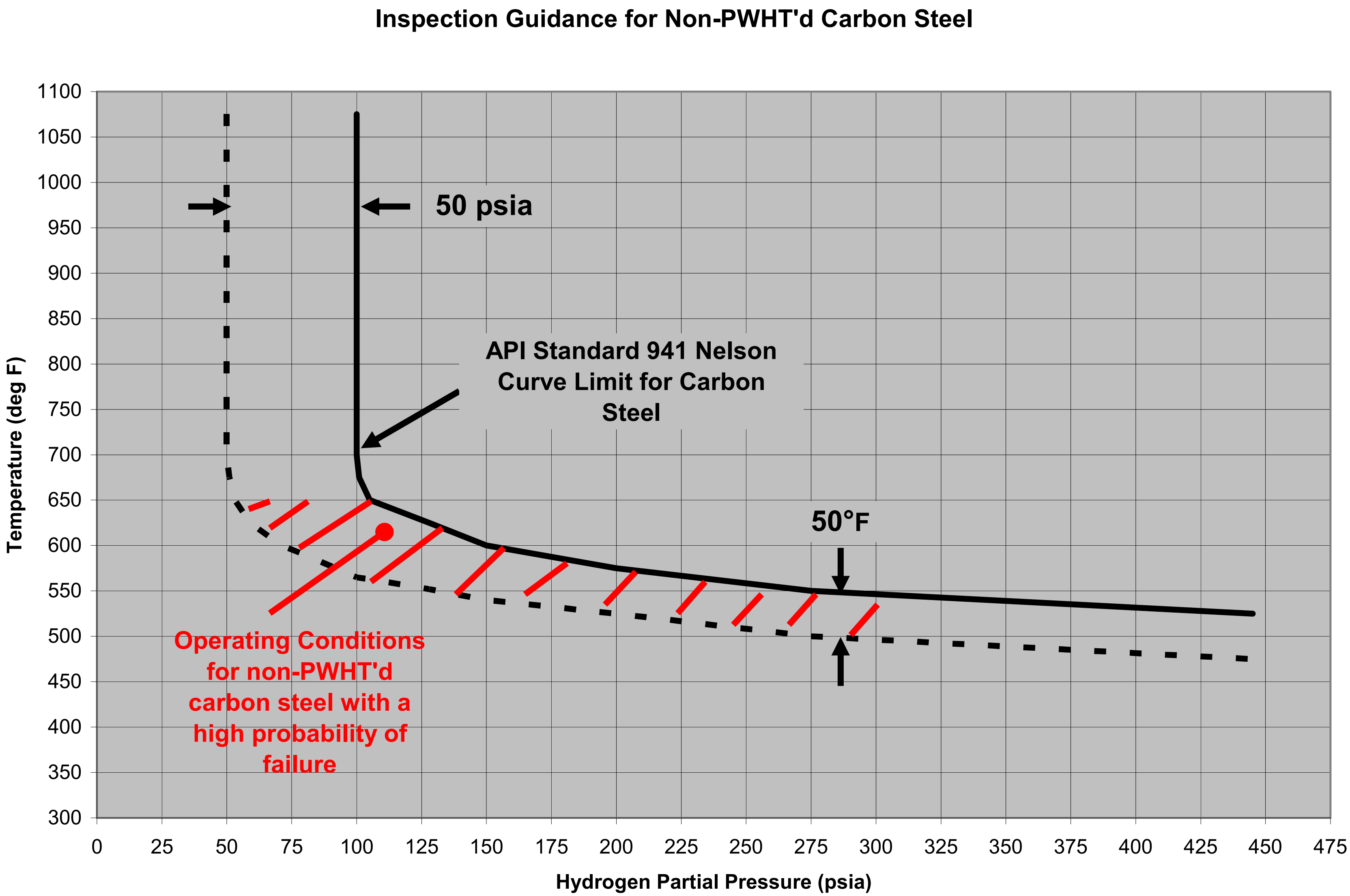

Appendix 8

Failure of the hydrogen recycle line of an HDS unit

(M. Richez)

FAILURE OF A HDS RECYCLE LINE

EFC WP 15 – MECHELEM – Martin RICHEz – TOTAL Refining & Chemical

FACTS

- HDS unit
- 29 October 2012 at 6H00 am rupture of the hydrogen recycle line
  - Unit emptied in about 20s
  - No fire, no explosion
  - Nobody outside
  - No fatality

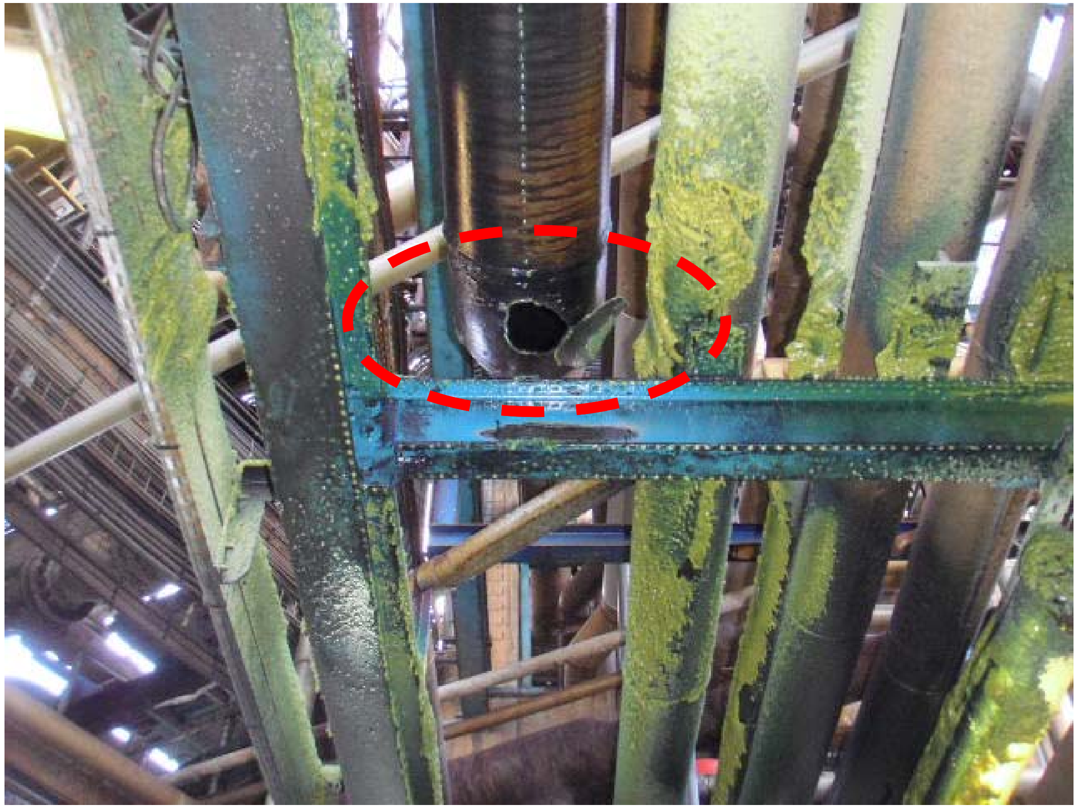

SIMPLIFIED SCHEME OF THE UNIT

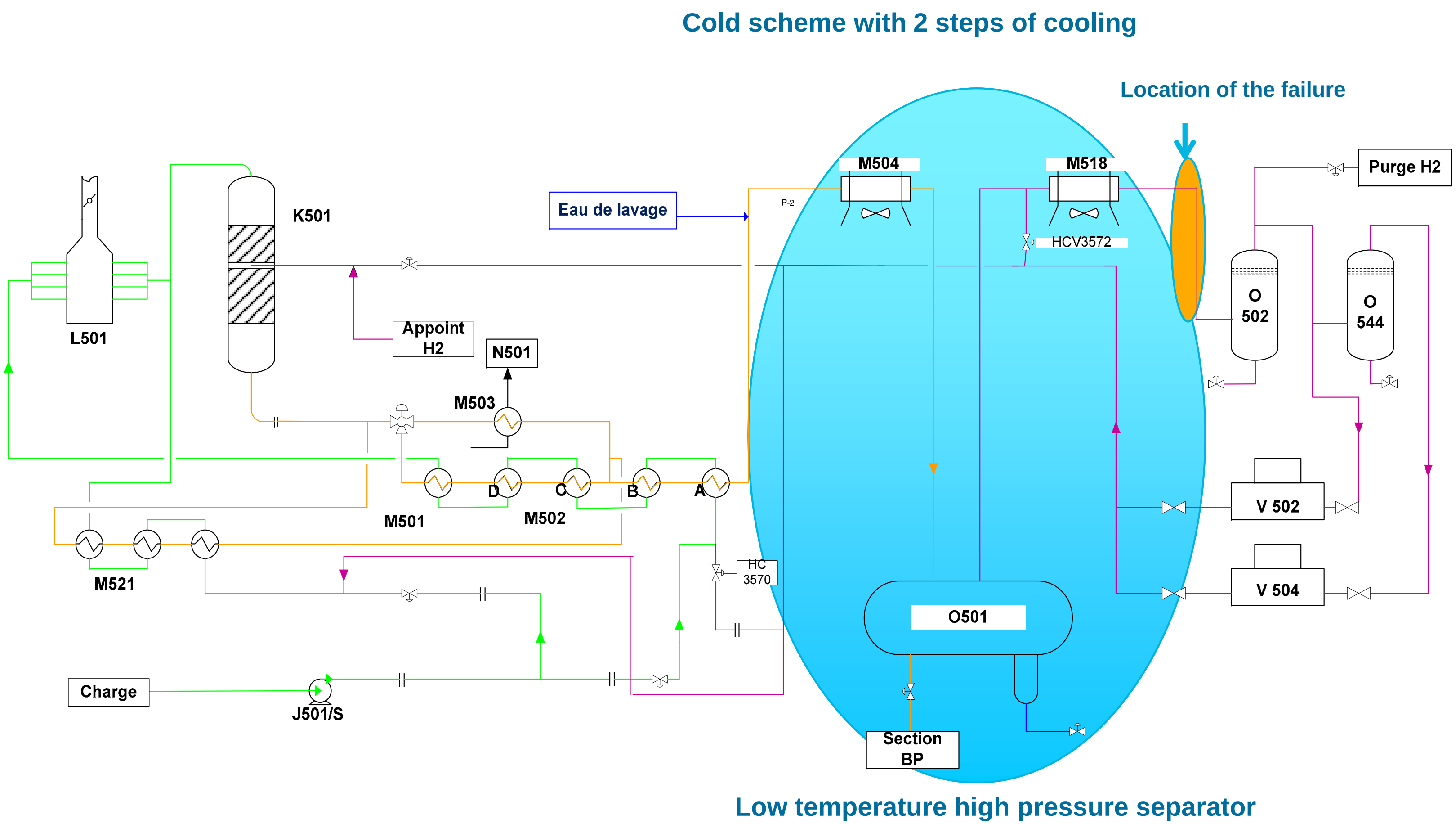

TOTAL

PIPING CHARACTERISTIC

- piping CS
- Diameter 10” (250 mm)
- Initial thickness 0.6” (15 mm)
- Piping installed in1989
- Unit from 1971
- Operating pressure around 650 PSI (45 bars)
- The failure happens in a 45° elbows
- Initial thickness measurements from 1997
- This elbows was measured in 2004 and 2007 without any significant loss
- only repair : in 1999 replacement of O 502 inlet (noted as erosion)

RESULT OF THICKNESS MEASURMENTS

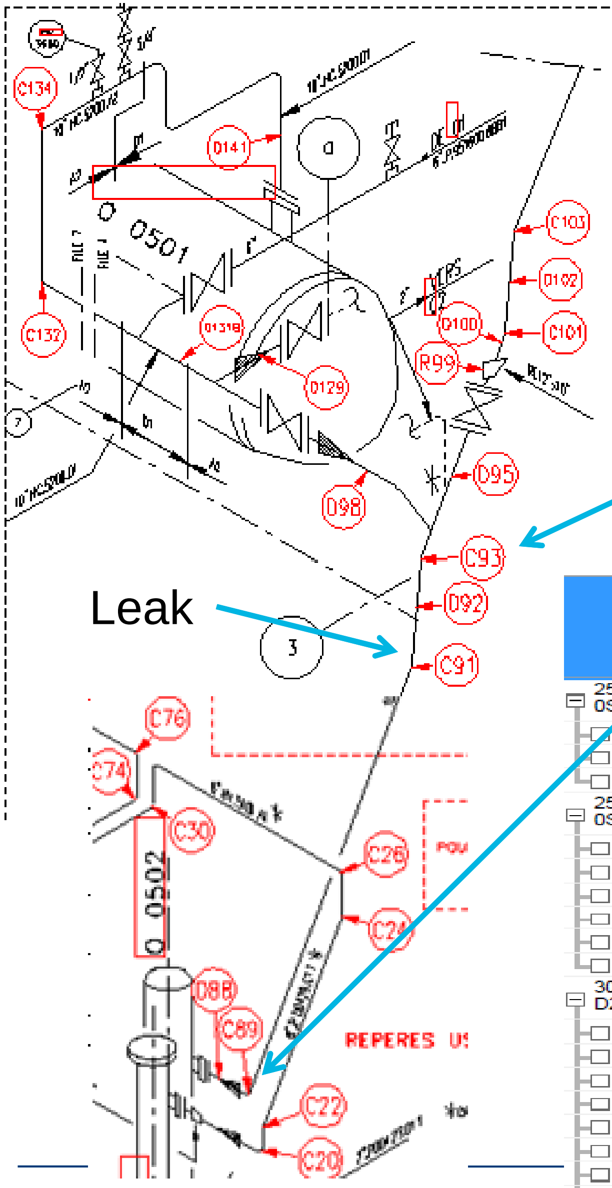

Significant thickness losses

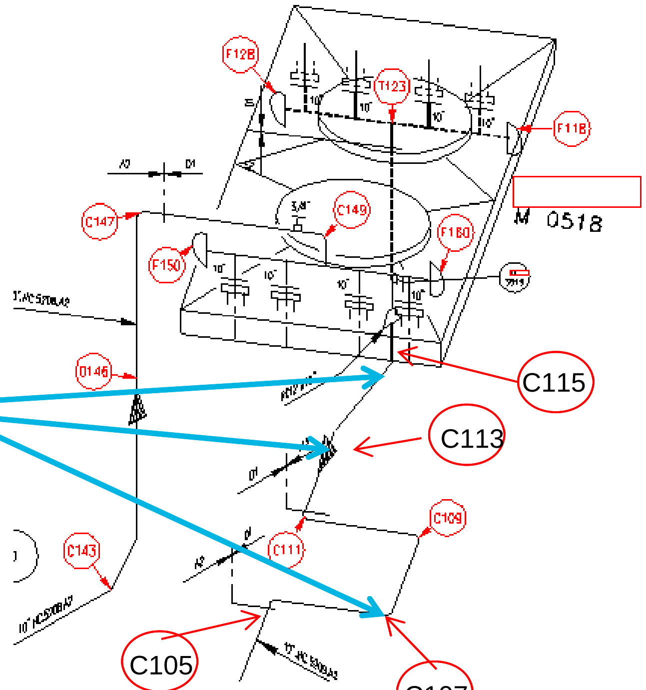

010 - Repère	Alarme 5 – Côte de remplacement	30 juin 1997	30 juin 1999	30 nov 1999	30 juin 2000	30 juin 2003	15 déc 2004	31 janv 2007	11 févr 2008	08 oct 2012
250P000421A2-HD2 0S003F0004										
D0095	4,85	15,30				15,20		15,00		14,50
D0098	4,85					16,00		15,20		15,60
R0099	4,85					14,70		16,50		21,40
250P000421D1-HD2 0S003F0004										
C0089	4,43	14,00	14,90	15,10	14,90		15,10	14,10		13,70
C0091	4,43						14,50	15,00		1,90
C0093	4,43		15,10		15,10		14,50	14,40		
D0088	4,43			15,10			15,50	14,60		14,20
D0092	4,43						13,30	13,80		13,50
S0512	4,45									
300HC005200A2-H D20S003F0004										
C0101	5,75		17,10		17,10	17,80			17,60	16,60
C0103	5,75					18,60			17,50	16,70
C0105	5,75									17,70
C0107	5,75									12,50
C0109	5,75								17,70	17,30
C0111	5,75						17,00	16,80		16,90
C0113	5,75									12,30
C0115	5,75									10,20
D0100	5,75					17,00		15,20		16,60
D0102	5,75					16,60			16,20	17,00

PICTURE OF THE RUPTURE ELBOW

Inside of tube (from the left)

inside of tube (from the right)

THICKNESS MEASUREMENTS OF THE FAILED ELBOW

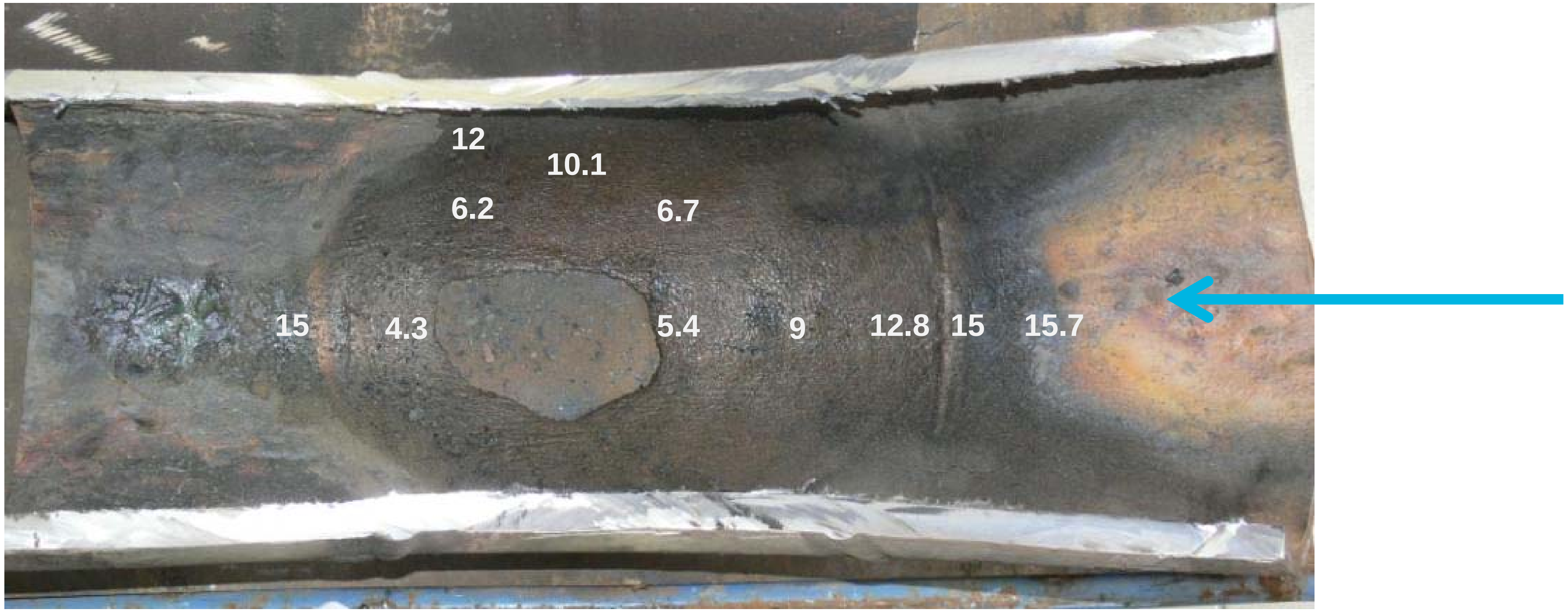

Nota: Les mesures sont exprimées en mm

Progressive thinning of the pipe up to the rupture area, where remaining thickness is about 0.08 » (2 mm).

SCHEMATIC REPRESENTATION OF THE DEGRADATION PROFIL

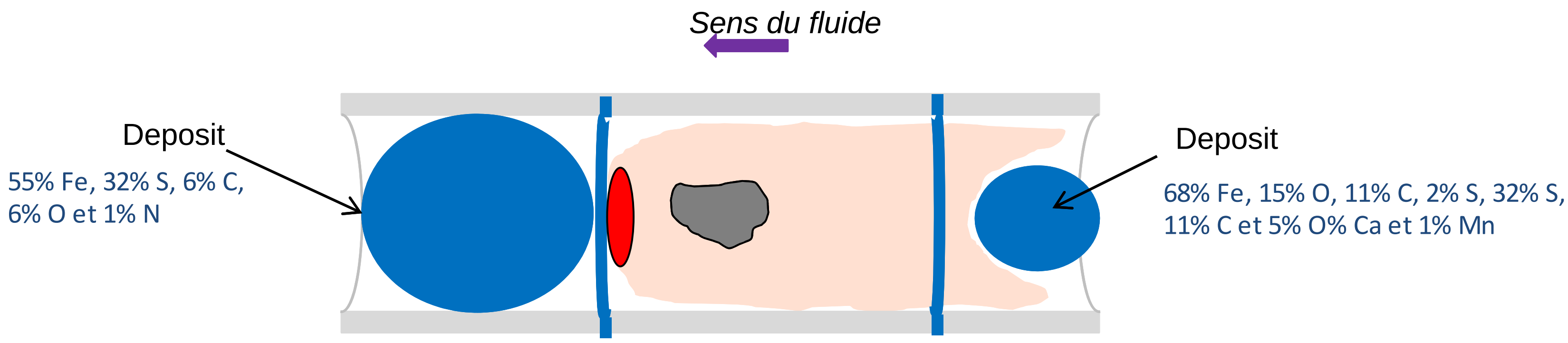

- Lack of deposit close to the rupture (rose area)
- Deposit foud upstream and downstream of the elbow (blue area) and mainly composed Fe and S. (to be noted, presence of N)
- The weld downstream the failure of the elbow present a thinner zone(read area)
- Around the rupture zone, the surface is rough with the presence of grooves
- It was concluded that the failure was due to erosion/corrosion by a solution of NH4HS

METALLOGRAPHIC EXAMINATION OF THE RUPTURE PART

2.7mm

PI*

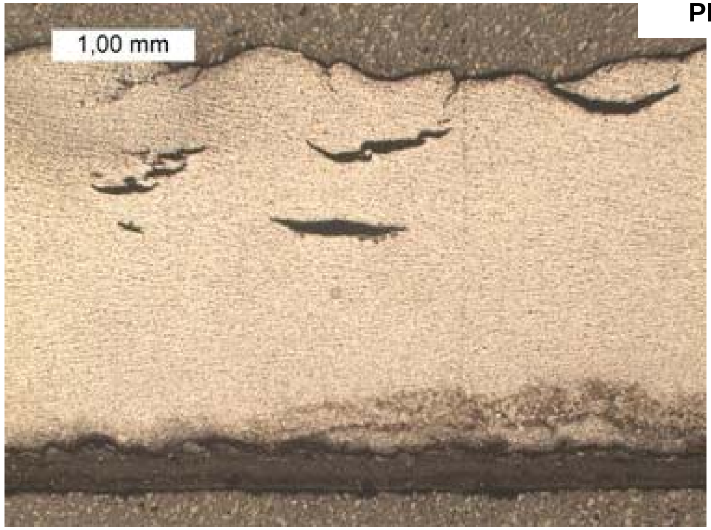

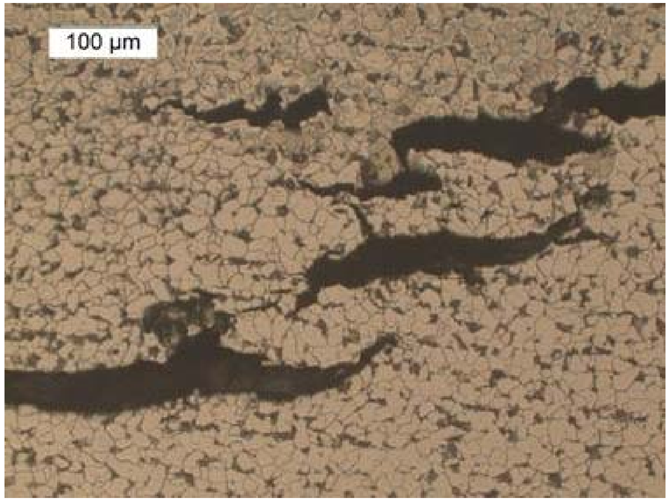

- presence of small blisters in the corroded area.
- <u>Typical of wet H2S damage</u>

*PI=peau interne

EXAMENS MÉTALLOGRAPHIQUES DU COUDE (1/3)

Sens du fluide

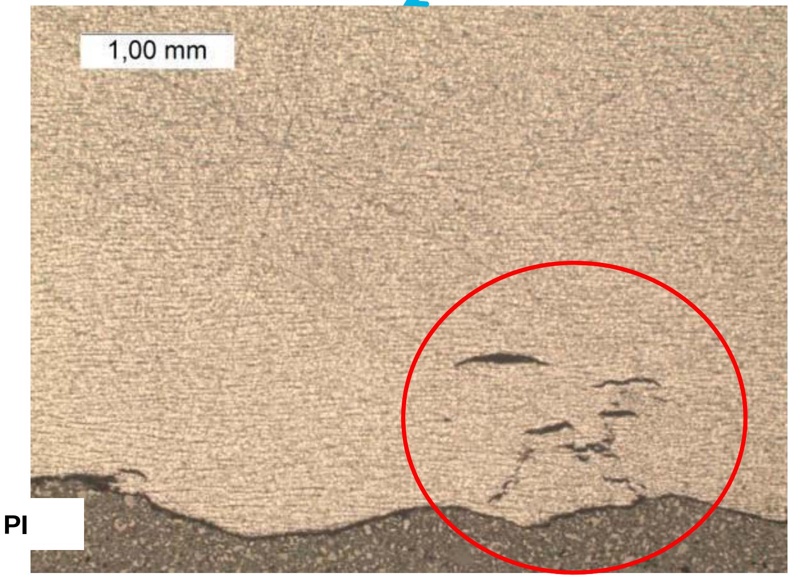

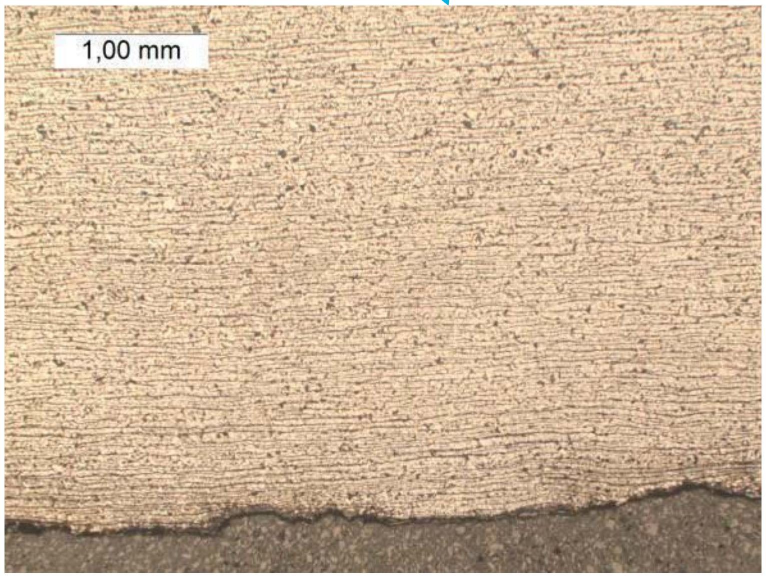

EXAMENS MÉTALLOGRAPHIQUES DU COUDE (2/3)

Sens du fluide

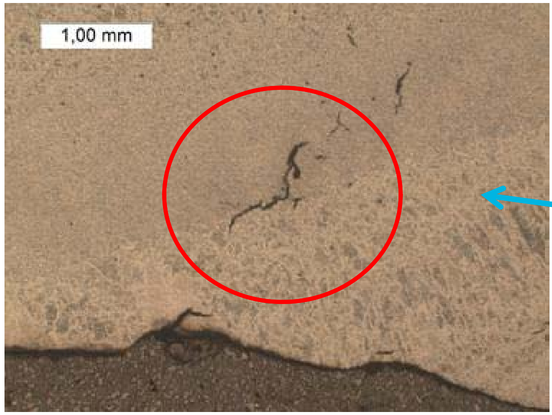

soudure

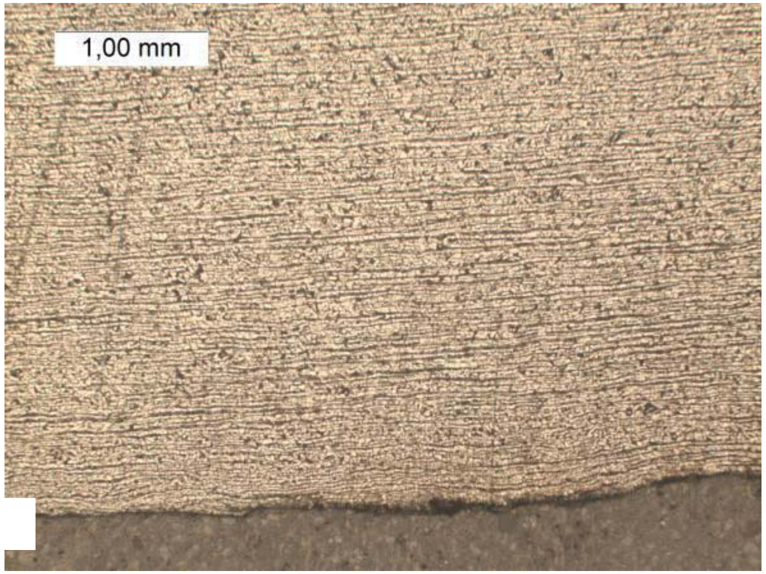

PI

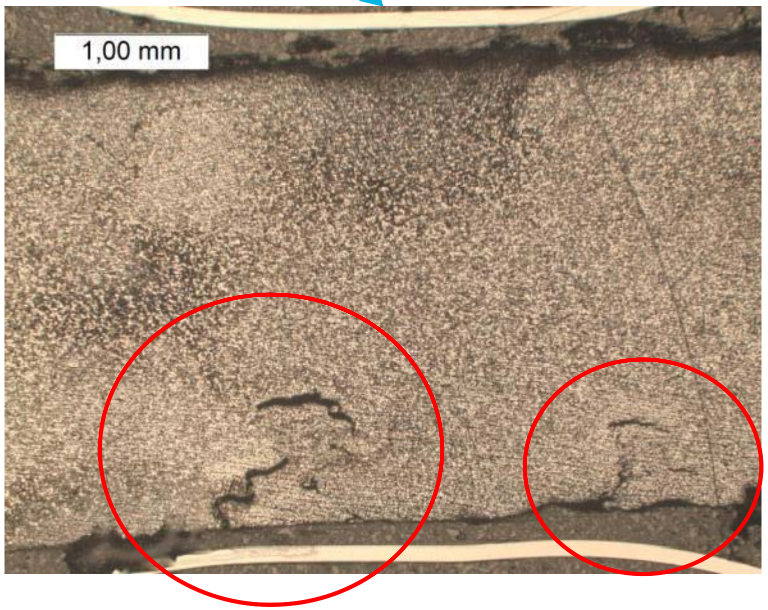

OPERATING CONDITION

Initialy design for processing GO in 1974

- Permanent water wash upstream of REAC
- HP separator operates between 40°C and 50°C
- H2S concentration in the gas phase 2.5 to 4 %
- NH4HS concentration in the boot is 5% max

Modification made in 1989 to process VGO (about 3 days per month)

- Addition of a second stage of air cooler (M 518) (second air cooler added in 1999)
- No water wash ahead of this air-cooler
- During VGO processing water wash upstream of REAC was stopped because the separator (O 501) is inefficient
- HP separator temperature is raised up to 70°C to avoid VGO freezing
- cooling in air cooler M 518 leads to water condensation
- If water condense NH4HS concentration in water reaches 45%
- H2S concentration in hydrogen is up to 12%
- Velocity is up to 45f ft/s (14 m/s)

API 932-B

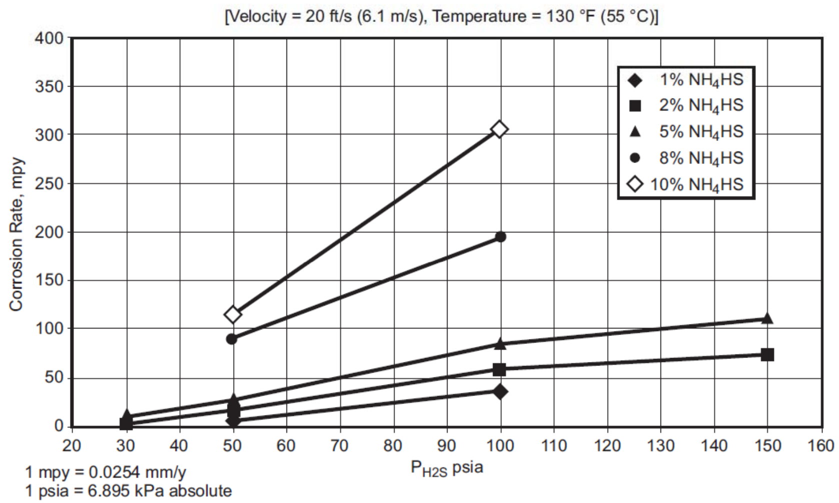

Figure 8—Curves Showing Effect of H_2S Partial Pressure on Corrosion of Carbon Steel

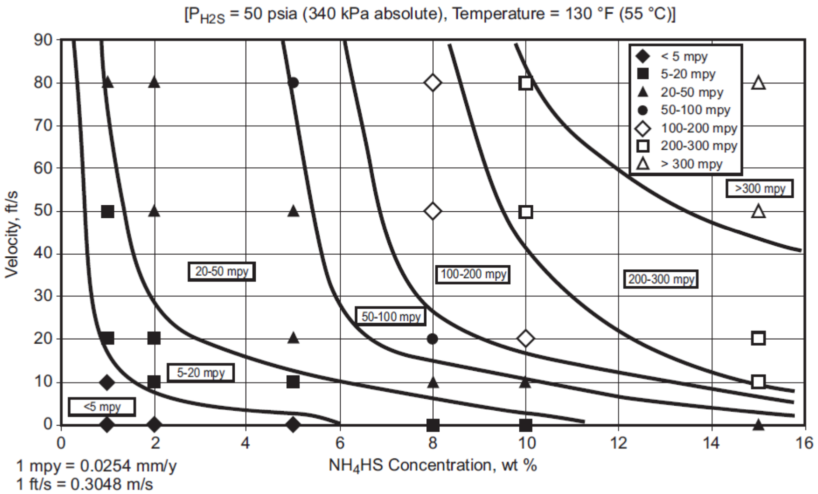

ORIGIN OF THE FAILURE

- When processing VGO a few water droplets will condense in AC M 518, with a high concentration in NH4HS, High H2S partial pressure, high velocity
- When processing GO, the conditions are less critical, but velocity is still high.
- When switching from VGO to GO, salt can be long to dissolve and NH4HS concentration may stay high for a long time
- Some factor are suspected to have increase the corrosion in the last years :
  - VGO tank temperature has been increase leading to higher water solubility
  - Tank agitator had been put in service and avoid water settlement
  - A leak was suspected on the water wash (which is turned-off when processing VGO)

An alert was sent to all TOTAL refineries

- Another unit had a similar scheme (about 1550 PSI)
- Original design of 1985 without any modification
- thickness measurement show that one elbow was already below minimum calculated thickness

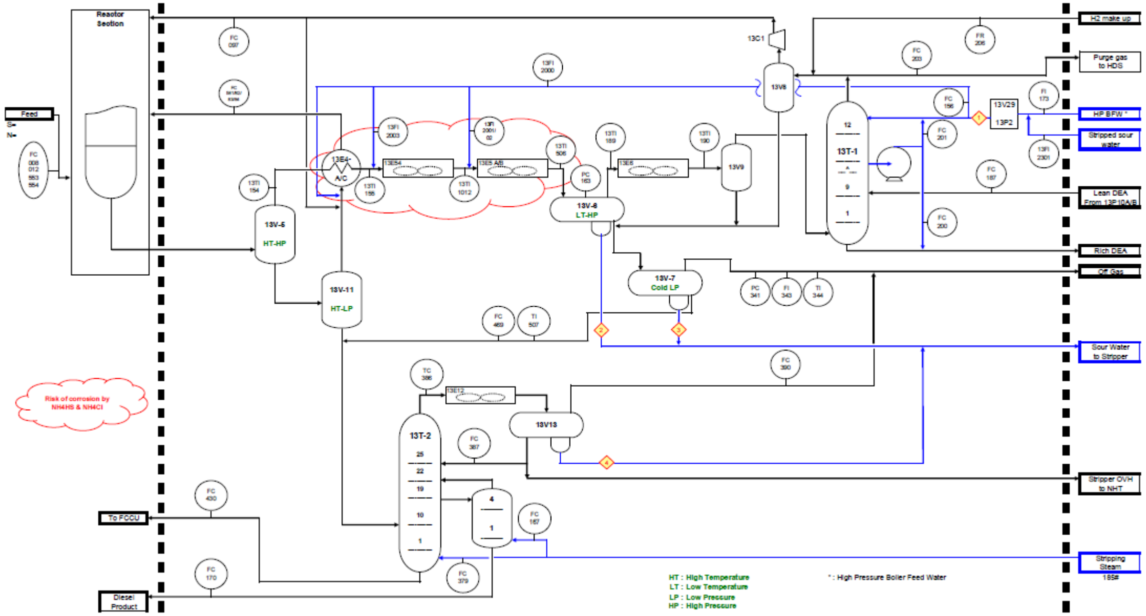

Appendix 11

Advances in high accuracy measurements in remote visual inspection

(C. Laverde, J. Van de Vijvere)

GE Inspection Technologies

Remote Visual Inspection (RVI)

Remote Visual Inspection Solutions for Oil & Gas Industry

Remote visual inspection in O&G industry can

- verify structural integrity
- reveal loose parts
- and identify potential problem areas.

RVI used at the beginning of shutdown help prioritize tasks by verifying asset health

RVI used at the end of an outage prior to closing out systems & equipment can

- verify system integrity
- verify absence of loose parts and dropped items

imagination at work

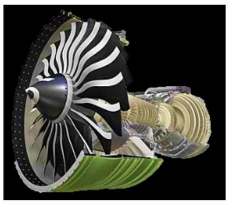

Remote Visual Inspection Applications

Static Equipment Applications

- Storage Tanks
- Heat Exchangers
- Cooling Towers
- Boilers
- Crude Units, Catalytic Cracker
- Fractionation Towers
- Spheres
- Cyclones
- Reactors
- Piping & Valves

Rotating Machinery Applications

- Gas Turbines
- Steam Turbines
- Compressors
- Pumps
- Fans
- Blowers

imagination at work

Inspected Static Equipment

	Video Probe XL GO+	Video Probe XL G3 w/ 3D Phase Measurement	PTZ Camera
Static Equipment			
Inspected equipement			
Heat Exchangers	YES	YES	NO
Cooling Towers	YES or XLVU+		
Boilers	YES	NO	NO
Pressure Vessels & Tanks	YES	NO	YES
Flow conditioners (Orifice Plates)	YES	YES	NO
Christmas Tree			YES
Piping	YES	YES	NO
Vessels	NO	NO	YES
Flanges	YES	YES	NO
Flex Risers	NO	NO	YES
Seals	YES	YES	NO
Valves	YES	YES	NO
Pumps	YES	YES	NO
Pre & Post Clean Exams	YES	YES	NO
Foreign Material Exclusion	YES	YES	NO
Ballast tanks	YES	YES	NO
Reactors	YES	YES	YES
Fin Fans	YES	YES	NO
Cyclones (oil & gas separation)	YES	YES	NO
Drain & Process Waste Lines	YES	YES	NO

imagination at work

imagination at work

Rotating Machinery Inspected Equipment

Equipment	Video Probe XL GO+	Video Probe XL G3 w/ 3D Phase Measurement
Turbine	NO	YES
Blowers	YES	YES
Compressors	YES	YES
Fans	NO	YES
Electric Motors	YES	YES
Pumping Systems	YES	YES
Hydraulic Units	YES	YES

imagination at work

5
GE Title or job number
4/17/2014

Downstream Showcase: Heat exchanger Petrochemical Plant (France)

XL Go VideoProbe

Concern:
Heat exchanger
diameter: 19.05 mm
Thickness: 11mm
length: 8m
Presents serious problems including corrosion and perforations

Solution:
RVI Inspection using the Video probe XLGo+ 8.4mm 8m
RVI can provide internal condition,

Value and cost saving:
- Rapidly assess damage mechanism for expedited corrective actions
- Instant RVI diagnosis with experiences can produce immediate repair/plug/bring in additional NDT technique decisions
- Use of RVI with experienced plant personnel can greatly reduce outage duration
- Inspection provides recordable, indexed, high quality documentation for review

imagination at work

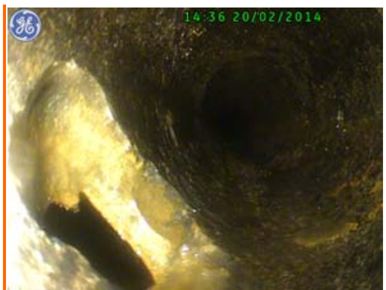

imagination at work

Downstream Showcase: Heat exchanger

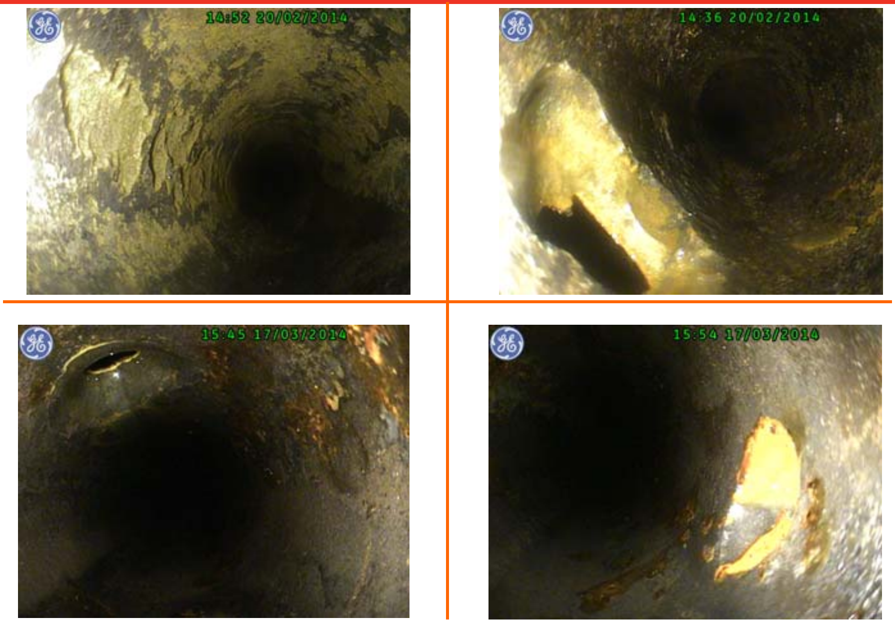

Downstream Showcase: Cooling Tower Refinery in UK

XL Go VideoProbe

Endoscope inspections of packing modules can provide an acceptable supplementary strategy and as such may be used to determine the need for pack removal for cleaning, or the cleaning of pack in-situ

imagination at work

Straightening vanes (Upstream Orifice Plate) Remote Visual Inspection)

XL Go VideoProbe

Scope view of straightening vanes. Observe the fouling on vane at the 9 o’clock position

Measurement errors can result if debris is trapped upstream of straightening vanes.

imagination at work

Tank and Vessel Remote Visual Inspection

Ca-Zoom

PTZ cameras for remote viewing in large Areas:
Tanks and Vessels Inspections, Weld Inspections, Corrosion Evaluation, Coke Drum Lining Inspection, Floating Roof Inspection, Fractionation Tower

imagination at work

Distillation Towers Remote Visual Inspection: Refinery in USA

Refinery Distillation Tower Inspection

imagination at work

Vessel Inspection / Weld Remote Visual Inspection

Chemical Company (Germany)

imagination at work

Turbine Remote Visual Inspection

XLG3 VideoProbe

3D Phase Measurement

Allows to find cracks, nicks, tears, missing material, deformations and to make 3D measurements.
Interactive Reporting

imagination at work

Centrifugal Compressor Remote Visual Inspection

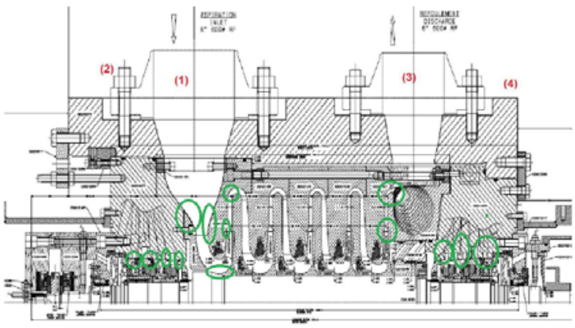

List of point of access for Boroscope inspection (in service) CENTRIFUGAL COMPRESSOR (OEM . THERMODYN) with OIL SEAL

GENERAL :

POA (Point of Access) is marked in RED COLOR (Number)

In GREEN COLOR is marked the area need to be inspected.

POA - ID	Probe suggest to be used + (F or S) view	Entrance point	Parts	Indication they normally found of CENTRIFUGAL COMPRESSOR
1	6 mm F	Inlet Flange	Diaphram / impeller	Erosion on surface and corrosion on Shaft do to the wet condition on the outage.
2	3,9 mm S	Hole of Oil supply (seal)	Shaft / Seal	Indication of # color is an indication of High Temp on the seal, evaluation of clearance ? presence of leakeage ?
3	6 mm F	Discharge Flange	Diaphram / impeller	Erosion on surface and corrosion on Shaft do to the wet condition on the outage.
4	3,9 mm S	Hole of Oil supply (seal)	Shaft / Seal	Indication of # color is an indication of High Temp on the seal, evaluation of clearance ? presence of leakeage ?

imagination at work

Steam Turbine Remote Visual Inspection

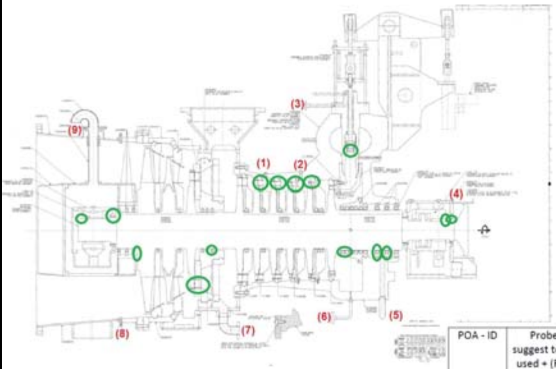

List of point of access for Boroscope inspection (in service) STEAM TURBINE (OEM . THERMODYN)

GENERAL :

POA (Point of Access) is marked in RED COLOR (Number)

In GREEN COLOR is marked the area need to be inspected.

POA - ID	Probe suggest to be used + (F or S) view	Parts	Indication they normally found of ST
1	5mm F	BLADE	Erosion on leading edge from Steam
2	5 mm F	BLADE	Erosion on leading edge from Steam
3	6 mm S	REG.VALVE	Erosion on VALVE on contact point between BASE/VALVE
4	3,9 mm S	SEALS	Indication of # color is an indication of High Temp on the seal, evaluation of clearance ? presence of leakeage ?
5	5 mm S	SEALS	Indication of # color is an indication of High Temp on the seal, evaluation of clearance ? presence of leakeage ?
6	3,9 mm S	SEALS	Indication of # color is an indication of High Temp on the seal, evaluation of clearance ? presence of leakeage ?
7	3,9 mm S	SEAL/BLADE?	Indication of # color is an indication of High Temp on the seal, evaluation of clearance ? presence of leakeage ?
8	3,9 mm S	SEAL	Indication of # color is an indication of High Temp on the seal, evaluation of clearance ? presence of leakeage ?
9	6 F/3,9S mm	SHAFT/SEAL	Indication of # color is an indication of High Temp on the seal, evaluation of clearance ? presence of leakeage ?

imagination at work

Thank you.

imagination at work

Appendix 12

Liquid insulation for Oil & Gas refining

(S. Reynolds)

Liquid Insulation Coatings

- Liquid insulation coatings have many desirable attributes for the Oil & Gas refining operations.
- Primarily, in the battle to minimise corrosion of asset infrastructure.
- In addition, & increasingly, to optimise plant operating efficiency
- This is presentation is an overview of recent developments in the field of improved performance materials.

Traditional Insulation

- “If someone could only come up with
- Jacketing that Doesn’t Leak
- And Insulation that Doesn’t Hold Water,
- we wouldn’t have all these
- Problems with Corrosion Under Insulation”
- Maintenance Manager’s Complaint

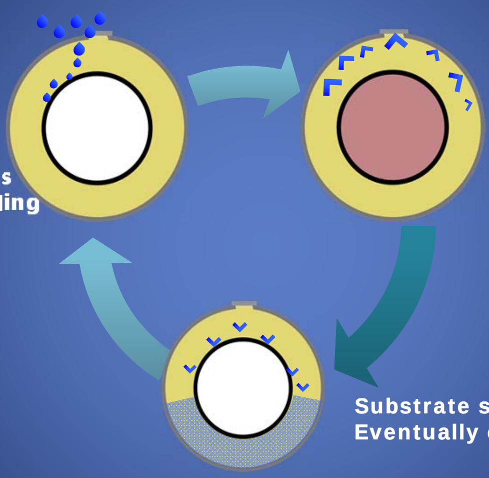

Problems with Traditional Insulation

- Installation & extended infrastructure costs.
- Complex shapes are difficult and expensive.
- Prone to physical damage and leakage.
- Wet Insulation doesn't insulate.
- Leaking insulation leads to severe corrosion.
- Modifications to system require disassembly.
- Insulation hinders ability to inspect equipment underneath.

Performance Polymers

Advantages of liquid insulation coatings ;

- Monolithic film totally encapsulating the object
- No leak paths for water to penetrate
- 100% Full adhesion to substrate limits corrosion potential
- Relatively low thickness' (<5mm)
- Easily maintained & repaired in situ
- Simultaneously provides thermal insulation & personal protection properties

Performance Polymers

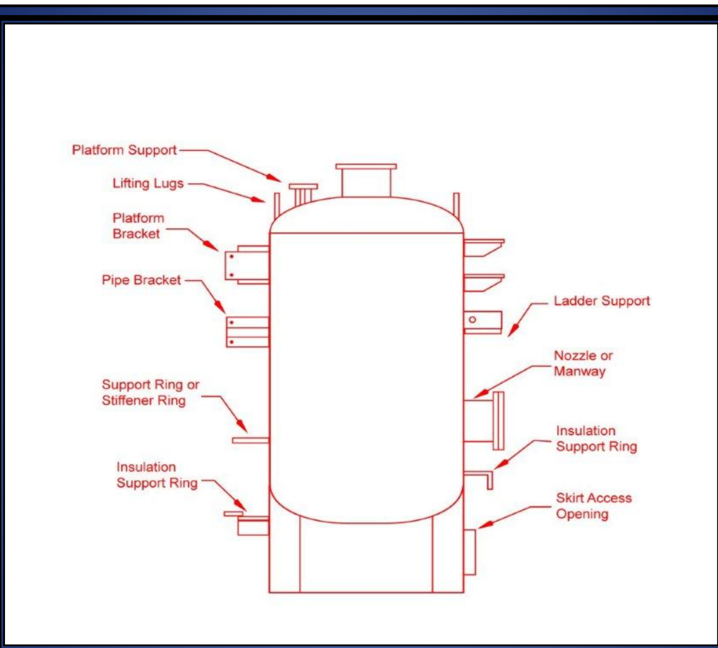

Current Technology

Within the insulative coatings arena, there traditionally have been two main additives promoted as providing an insulation benefit: glass and ceramic spheres. These are hollow in nature, and trap a small amount of air inside. This trapped air can be considered “still” in nature, and contribute an impressive thermal conductivity of 26mW/mK.

Factoring in the glass or ceramic shell that holds the air, individual spheres in the range of 50–200 mW/mK are easily produced in a variety of sizes and wall thicknesses. When mixed with paints at high loadings, they can achieve an overall thermal conductivity of 70+ mW/mK.

Thermal Insulation with Glass or Ceramic beads

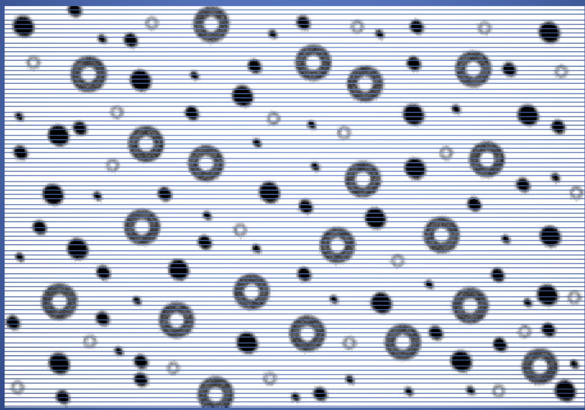

Limitations

- Multiple applications required to achieve optimal thermal efficiency
- Significantly higher applied costings
- Temperature resistance currently 180’C
- Coatings vulnerable to performance degradation due to fragile nature of fillers both in application & cyclic service.

The Next Generation

Aerogels

Aerogels are a synthetic, porous ultralight material derived from a gel, in which the liquid component of the gel has been replaced with a gas. The result is a solid with extremely low density and low thermal conductivity. Nicknames include "frozen smoke“, "solid smoke", "solid air" or "blue smoke" owing to its translucent nature and the way light scatters in the material

Despite their name, aerogels are solid, rigid, and dry materials that do not resemble a gel in their physical properties: The name comes from the fact that they are made from gels it is very strong structurally. Its impressive load bearing abilities are due to the dendritic microstructure, in which spherical particles of average size (2–5 nm) are fused together into clusters. These clusters form a three-dimensional highly porous structure of almost fractal chains, with pores just under 100 nm. The average size and density of the pores can be controlled during the manufacturing process.

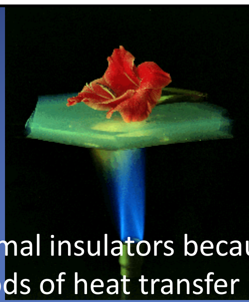

Aerogels are good thermal insulators because they almost nullify two of the three methods of heat transfer (convection, conduction, and radiation). They are good conductive insulators because they are composed almost entirely from a gas, and gases are very poor heat conductors. Silica aerogel is especially good because silica is also a poor conductor of heat (a metallic aerogel, on the other hand, would be less effective). They are good convective inhibitors because air cannot circulate through the lattice.
The term aerogel does not refer to a particular substance, but rather to a geometry which a substance can take on–the same way a sculpture can be made out of clay, plastic, papier-mâché, etc., aerogels can be made of a wide variety of substances.

Performance Polymers

Silica Aerogels

- Highly porous
- > 90% Pores (air)
- Density 30 – 100 kg/m^3
- Best thermal insulating solid
  12 mW/mK
- Highly hydrophobic grades available on an industrial scale

Performance Polymers

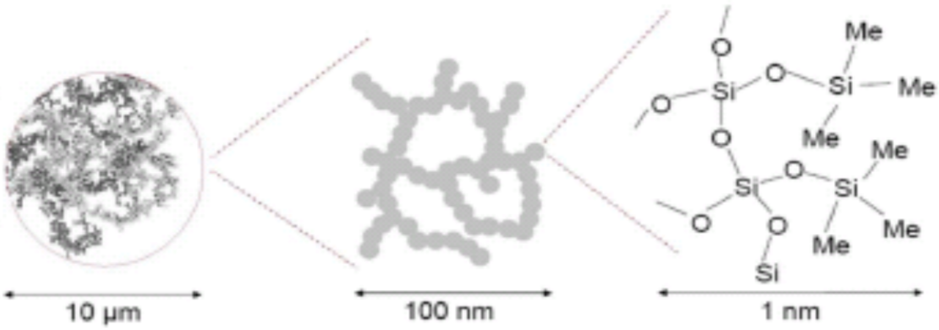

Silica Aerogels

Nano-sized pores: the key factor for insulation

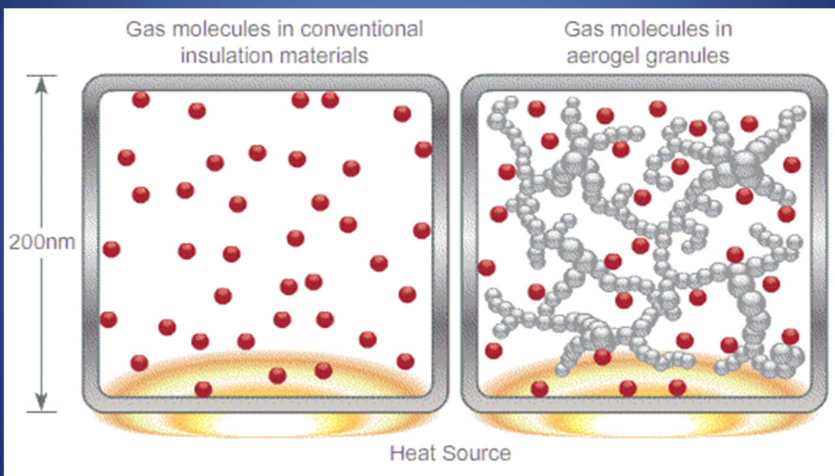

Silica Aerogels

Comparison of Thermal Conductivity

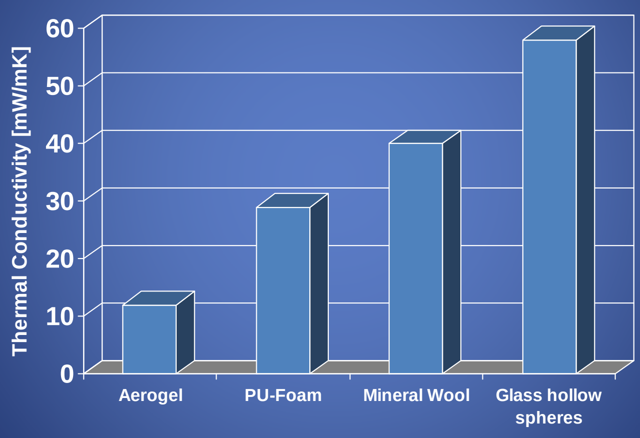

Insulating properties

7-10x More insulating than typical paint

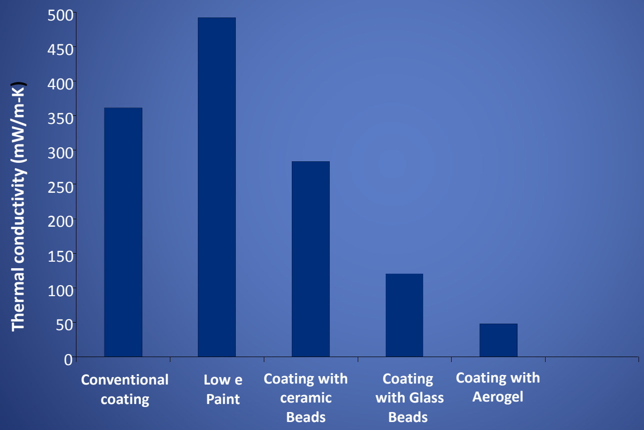

TABLE 1 | Thermal properties of insulative coatings.

Acrylic Coating	Insulation Technology	Approximate Thermal Conductivity (mW/m-K) (BTU/hr-ft-°F)	Average Application Thickness – One Coat (mm/mils)	Thermal Resistance per Pass ($x10^3 m^2K/W$)
A	Aerogel	35/0.02	1.5/60	42.9
B	Ceramic microspheres	70/0.04	0.5/20	7.1
C	Ceramic microspheres	100/0.06	0.375/15	3.8
D	Ceramic microspheres	100/0.06	0.375/15	3.8
E	None	300/0.17	0.1/4	0.3

SAFE TOUCH

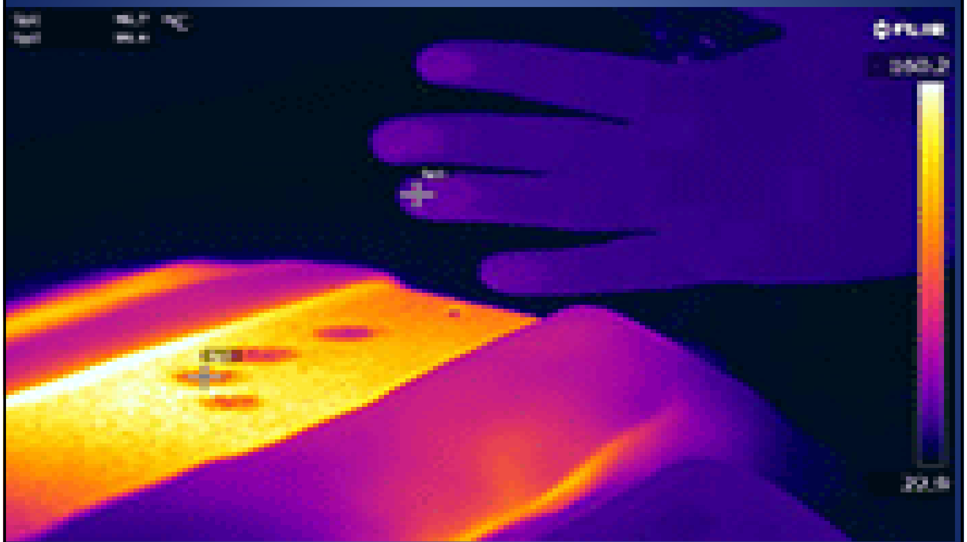

Thermaguard 180

- Combination of hydrophobic Aerogels with special water based binders
- Water based Acrylic dispersions
  - Special modifications for incorporation of Aerogels
  - 1-K System
  - High elasticity even at low temperatures
  - Excellent adhesion to various substrates
- Binders and additives adjust properties for various performances
  - Rheology modification for spraying, rolling or knife application
  - Flame retardant properties

Performance Polymers

Thermaguard 180

- Sprayable thermal insulating coating
- Low thermal conductivity
- Low heat capacity
- Excellent adhesion
- 1K waterbased binder system
- Ambient temperature drying
- No solvents
- Logistically classified as Non Hazardous

Performance Polymers

Thermaguard 180

Wet Formulation	
Density	approx. 0,5 g/cm³
pH-Value	8,3 – 8,5
Solids	approx. 67,0 %
Water-content	approx. 32,0 %
Dried Coating	
Hardness	30 – 40 Shore A
Coverage for 1mm dry film, 1,2 mm wet film	540 g/m²
Max. film thickness	approx.30 mm
Thermal conductivity	approx. 46 mW/mK
Water vapor transmission rate (8 mm thickness) sd-value (diffusion equivalent air layer thickness)	**25 g/m²d** **0,76m (Class V_2 acc. DIN EN 1062-1)**

Performance Polymers

Developments in binder technology

With the development of Polysiloxanes, coating systems composed of inorganic polymers have been introduced to the Protective Coatings Ind**ustry.**

High build, high solids polysiloxane hybrid resins are essentially cold applied ceramic compounds. the polymeric structures of these polysiloxanes have much in common with the three dimensional silicon-oxygen structure of quartz.

ESSENTIALLY BECAUSE OF THE INORGANIC SILICON – OXYGEN BACKBONE, THEY HAVE NONE OF THE FAILURE CHARACTERISTICS OF ORGANIC COATINGS.

Performance Polymers

Polysiloxane technology

This has resulted in the introduction of acrylic & epoxy polysiloxanes hybrid binders, and has caused a breakthrough in the protective coatings industry.

By the combination of acrylic/epoxy organic and siloxane based inorganic binder systems, high technology coatings have been introduced providing the durability and toughness of epoxy coatings whilst outranking the gloss and colour retention of the best urethane based topcoats.

Thermaguard 350

Incorporation of Aerogel & Siloxane technologies yields fascinating possibilities of a new spectrum of materials that will be able to push the operating boundaries to new highs.

Exception thermal & physical performance is now extending thermal insulation coatings to 350'C continuous operating temperatures and beyond, whilst additionally providing for extended service life projections.

Applicable Standards:

Thermal Properties:

ASTM G154 UV EXPOSURE
ASTM C177 THERMAL TRANSMISSION
ASTM C236 THERMAL CONDUCTANCE
ASTM C411 PERFORMANCE OF INSULATION
ASTM E971 TRANSMITTANCE
ASTM C1055 HEATED SYSTEM SURFACE
ASTM C1057 SKIN CONTACT
ASTM E1175 SOLAR REFLECTANCE
ASTM E1269 SPECIFIC HEAT CAPACITY
ASTM C1363 THERMAL PERFORANCE
ASTM C1371 EMMITANCE
ASTM E1461 FLASH METHOD
ASTM C1549 SOLAR REFLECTANCE

Performance Polymers

Physical Properties
ASTM G53 ACCELERATED WEATHERING
ASTM E84 SMOKE/FLAME SPREAD
ASTM G96 WATER VAPOR TRANSMISSION
ASTM B117 SALT SPRAY TEST
ASTM D412 TENSILE PROPERTIES
ASTM D522 MANDREL BEND
ASTM D638 ELONGATION RATE
ASTM D1653 WATER VAPOR TRANSMISSION
ASTM D3273 FUNGAL RESISTANCE
ASTM D3274 FUNGAL RESISTANCE
ASTM D3359 CROSS HATCH ADHESION
ASTM 4060 ABRASION RESISTANCE
ASTM D4541 PULL APART STRENGTH
ASTM D4585 HUMIDITY CABINET
ASTM D4587 UV EXPOSURE
ASTM D5894 UVA EXPOSURE

Performance Polymers

Thermaguard 650 ++ ?

Thank You